Identification Report: Earthquake Test on 2-Bay, 6-Story Scale 1:5 RC-Frames

Kirkegaard, Poul Henning; Skjærbæk, P. S.; Nielsen, Søren R. K.

Publication date:
1997

Document Version
Early version, also known as pre-print

Link to publication from Aalborg University

Citation for published version (APA):
Kirkegaard, P. H., Skjærbæk, P. S., & Nielsen, S. R. K. (1997). *Identification Report: Earthquake Test on 2-Bay, 6-Story Scale 1:5 RC-Frames*. Dept. of Building Technology and Structural Engineering, Aalborg University. Fracture and Dynamics Vol. R9703 No. 85

INSTITUTTET FOR BYGNINGSTEKNIK
DEPT. OF BUILDING TECHNOLOGY AND STRUCTURAL ENGINEERING
AALBORG UNIVERSITET • AAU • AALBORG • DANMARK

FRACTURE & DYNAMICS
PAPER NO. 85

P. H. KIRKEGAARD, P. S. SKJÆRÆK & S. R. K. NIELSEN
IDENTIFICATION REPORT: EARTHQUAKE TESTS ON 2-BAY, 6-STOREY SCALE 1:5 RC-FRAMES
MARCH 1997 ISSN 1395-7953 R9703

Printed at Aalborg University

Identification Report: Earthquake Tests on 2-Bay, 6-Storey Scale 1:5 RC-Frames

P.H. Kirkegaard, P.S. Skjærbæk & S.R.K. Nielsen

Aalborg University
Department of Building Technology and Structural Engineering
Sohngaardsholmsvej 57, DK-9000 Denmark

CONTENTS

1 INTRODUCTION

The aim of the present report is to supply the identification results from the tests performed with a laboratory model of a plane 6-storey, 2-bay scale 1:5 RC-frame at Aalborg University, Denmark during the autumn 1996. The tests were performed as a part of a Ph.D. study considering evaluation of damage in RC-structures submitted to strong motion excitation. The details of the tests and the construction of the frame, respectively are presented in a report , Skjærbæk et al. [1] describing the experimental test programme.

The tests were performed with three set-ups named AAU1, AAU2 and AAU3, respectively. Each of these set-ups was dynamically tested by pull-out excitation, weak earthquake excitation and strong earthquake excitation. These different tests have been used to estimate the modal parameters of the undamaged as well as the damaged structure. Before the model was subjected to the strong earthquake excitation free-decay tests and weak motion excitation were performed. For set-up AAU2 and AAU3, these free-decay test were performed with three different pull-out forces. After the tests of the undamaged structure an earthquake excitation was subjected to the structure. Artificial earthquakes giving an excitation in the first mode for AAU1 and AAU2, and in the second mode for AAU3, respectively were used. After the earthquake test pull-out test were performed again.

In order to analyse the measured time series well-proved system identification techniques have been used. The free-decay time series were analysed by means of the ARV, ERA, Polyreference and ARMAV techniques, see e.g. Pandit [2], Juang [3], Vold [4], Kirkegaard et al. [5]. The time series from the earthquake tests were analysed using a recursive time domain implementation of the ARMAV technique, Kirkegaard et al. [5]. Only the two lowest bending modes in the plane will be considered in the identification process.

The report is organized in 6 chapters. Chapter 2 shortly presents the RC- frame and test equipment. Thereafter 3 chapters are following, presenting the results from frame AAU1, AAU2, and AAU3, respectively. The results are summarised in chapter 6 and comments to the results are given. At last in chapter 7 and 8, respectively acknowledgements and references are given.

2. PRESENTATION OF RC-FRAME AND MEASURED DATA

This section gives a short presentation of the test frame and test set-up. For a detailed description of the structure and data acquisition system, see Skjærbæk et al. [1].

2.1 Description of Frame Structures AAU1, AAU2 and AAU3

All the 6 frames considered in the test series were constructed identically. The test frames considered are 6-storey, 2-bay RC-frames. The dimensions of the test frames are 2400 by 3300 mm. Corresponding to a "real" structure with dimensions 12 by 16.5 m. The test frame is build of 50 by 60 mm RC-sections reinforced with 6 mm KS410. A plane view of the test frame is shown in fig. 2.1. The weight of each frame is approximately 200 kg. To model the storey deck, 8 RC beams (0.12*0.12*2.0m) are placed on each storey. The total mass per frame is then 2000 kg. The experimental set-up is shown in figure 2.2. The frames were tested in pairs of two, where the storey weights are modelled by placing the RC-beams in span between the two frames. Each of the two frames were instrumented with Brüel & Kjær and Kistler accelerometers at each storey, see figures 2.6 and 2.7. The excitation of the structure was performed in two ways. Either by moving the shaking table as illustrated in figure 2.2 or by applying a force at the top storey which was suddenly released by cutting a thin thread as illustrated in figure 2.5. However, AAU1 was free-decay tested by means of a rope attached to the top storey beams.

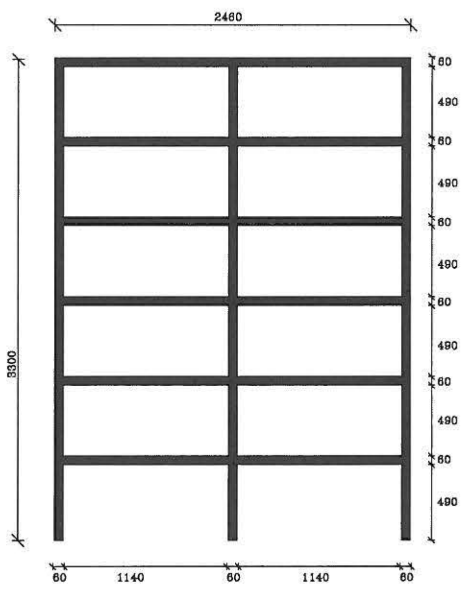

Figure 2.1 : Plane view of test frame

All longitudinal reinforcement, see figure 2.3 , used in the frame are of the type KS410 (ribbed steel) with a characteristic (2 % fractile) yield stress of 410 MPa . In table 2.1 the yield f_y, the ultimate $_{du}$ and the modulus of elasticity E_s are listed for three reference specimens of the used reinforcement bars.

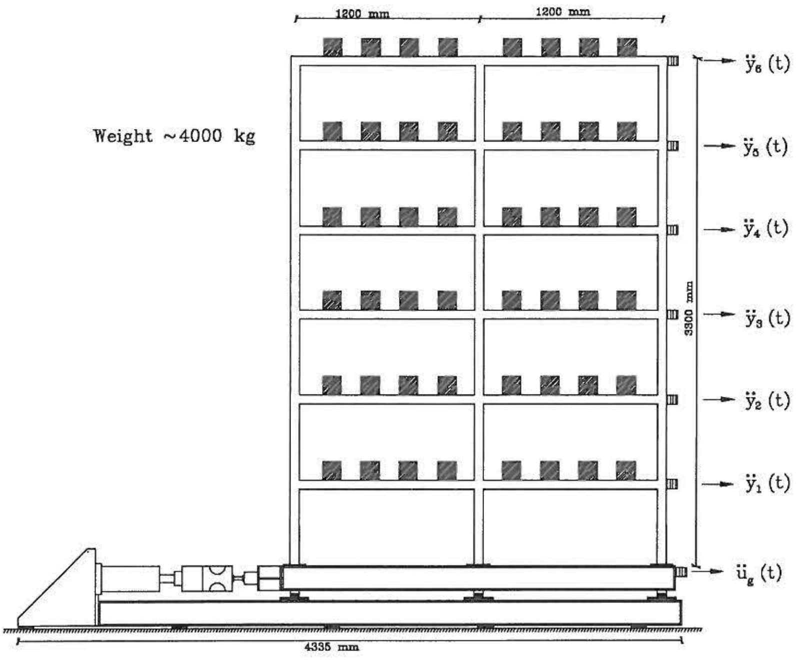

Figure 2.2 Experimental set-up of the test frames.

To avoid overlapping longitudinal reinforcement causing uncontrolled changes in bending stiffness and strength the longitudinal reinforcement bars are ended with anchoring steel-plates welded to the reinforcement. The concrete used has a design compression strength of 20 MPa with a maximum aggregate diameter of 5 mm. For each frame is used approximately 80 l concrete. The columns in the lower storey are reinforced for shear with 3mm steel thread which has been formed into spirals.

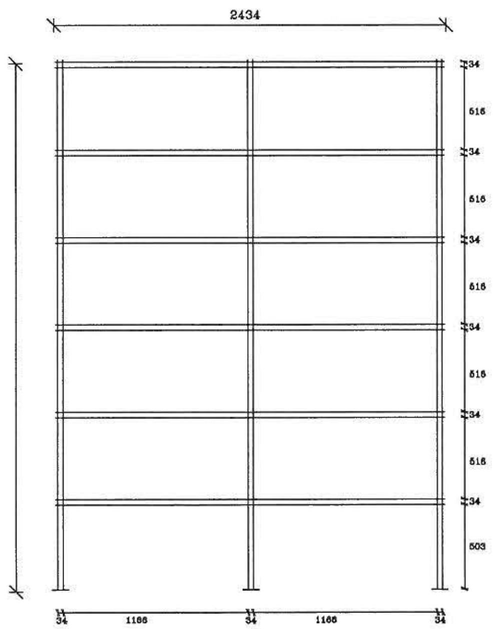

Figure 2.3 Main reinforcement in frame. All measures in mm.

The dimensions of the beams and columns in the frame are constant all over the frame with outer measures of 50 × 60 mm. Columns are reinforced with 6 6 mm KS410 (ribbed steel) and beams with 4 6 mm KS410, see figure 2.4.

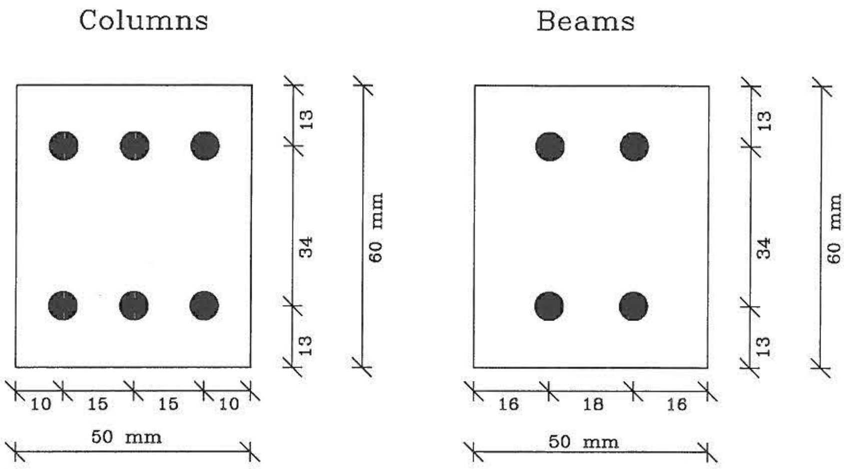

Figure 2.4 Cross-section of beam and columns.

Test Specimens No.	f_y [MPa]	f_{su} [MPa]	Es *10 ^5 [MPa]
1	535	642	2.003
2	535	644	1.842
3	542	650	2.013

Table 2.1 Steel parameters from three reference specimens of the used reinforcement bars.

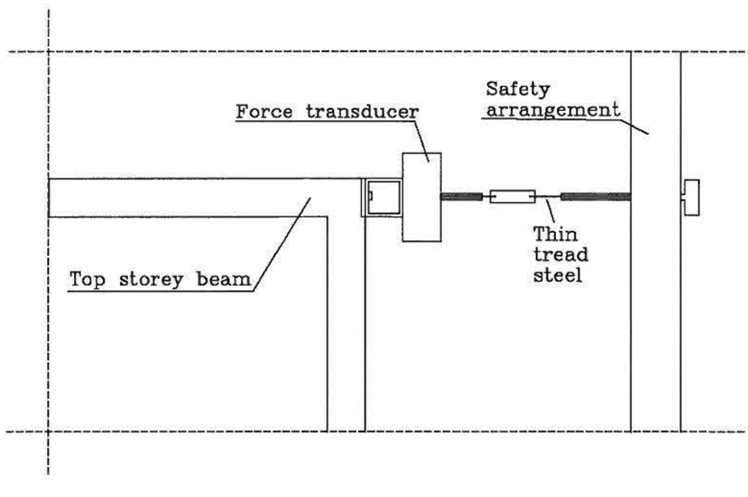

Figure 2.5 Excitation setup used for free-decay tests of AAU2 and AAU3.

In all the three set-ups AAU1, AAU2 and AAU3 each of the two frames in the set-up was installed with accelerometers. Set-up AAU1 was installed as shown in figure 2.6 with accelerometers at all storeys on one of the frames an accelerometers on the 2nd, 4th and 6th storey of the other frame. Furthermore, displacement transducers were present at the top-storey on both frames. Two accelerometers (15) and (16) in figure 2.6 measured the out of plane accelerations. The instrumentation of AAU2 and AAU3 was different from the one of AAU1, so accelerometers were present at all storey of both frames.

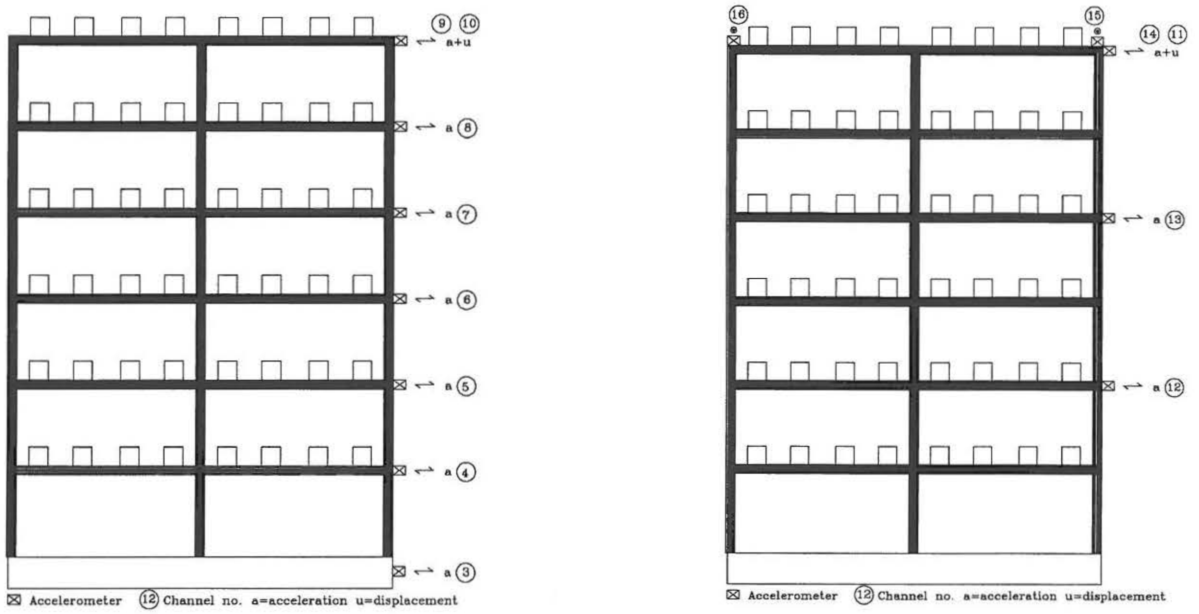

Figure 2.6 Instrumentation for frame AAU1.

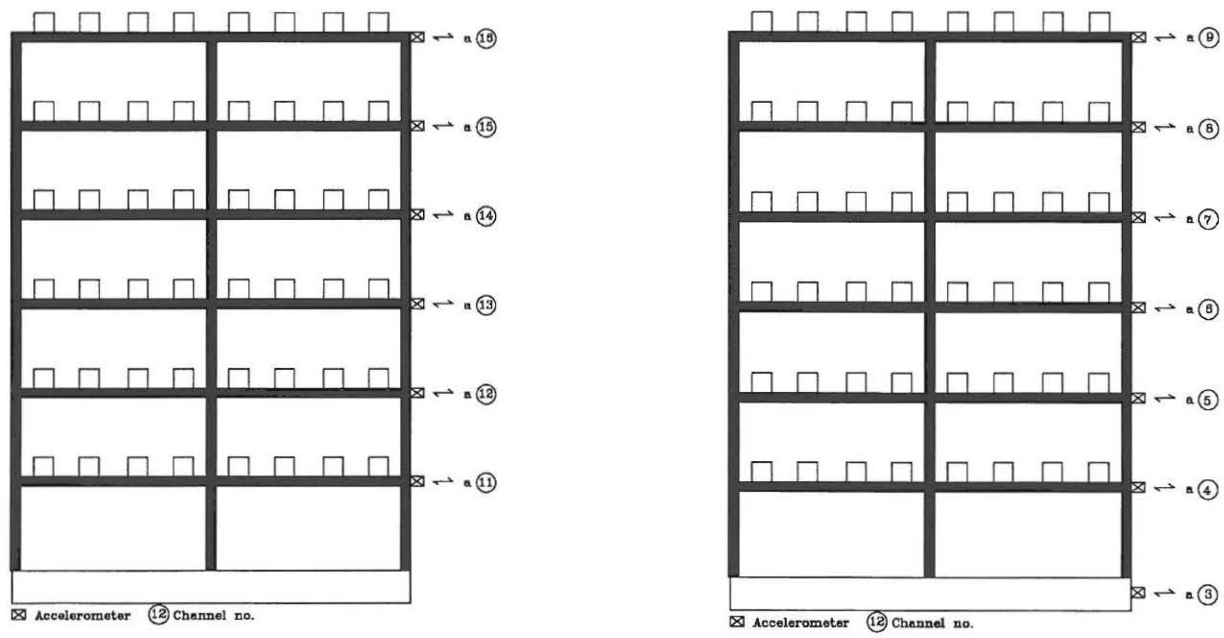

Figure 2.7 Instrumentation for frame AAU2 + AAU3.

3 ANALYSIS OF TESTS MEASUREMENTS FROM FRAME AAU1

In this chapter the results from the system identification of frame AAU1 are presented.

3.1 Description of test data from frame AAU1

The files with the data from the performed tests with frame AAU1 are named in table 3.1.

Name	Case
fd1_b00.dat	Free decay in the plane, No. 0. (before accident)
fd1_b01.dat	Free decay in the plane, No. 1.
fd1_b02.dat	Free decay in the plane, No. 2.
fd1_b03.dat	Free decay in the plane, No. 3.
fd1_r01.dat	Free decay in rotation, No. 1.
fd1_r02.dat	Free decay in rotation, No. 2.
fd1_r03.dat	Free decay in rotation, No. 3.
wm1_ta01.dat	Type a earthquake with intensity 1 % of max.
wm1_tb01.dat	Type b earthquake with intensity 1 % of max.
wm1_tc01.dat	Type c earthquake with intensity 1 % of max.
sm1_25a.dat	Strong motion earthquake EQ1 (type a) with intensity of 25 % of max.
wm1_1a1.dat	Weak motion earthquake of type a with intensity of 1 %. After EQ1
fd1_b04.dat	Free decay in the plane, No. 4.
fd1_r04.dat	Free decay in rotation, No. 4.
sm1_50a.dat	Strong motion earthquake EQ2 (type a) with intensity of 50 %of max.
wm1_1a2.dat	Weak motion earthquake of type a with intensity of 1 %. After EQ2
fd1_b05.dat	Free decay in the plane, No. 5.
fd1_r05.dat	Free decay in rotation, No. 5.
sm1_75a.dat	Strong motion earthquake EQ3 (type a) with intensity of 75 % of max.

Table 3.1 Test data from frame AAU1.

From table 3.1 it is seen that 11 free decay measurements, 5 weak motion measurements and 3 strong motion measurements were performed. Three free decay and three weak earthquake tests were performed before the first strong earthquake test in order to make a virgin state identification of the frame. The free-decay tests were performed by means of a rope attached to the top storey beams. The following measurement sessions consisted of one strong motion measurement, one weak motion measurement and 2 free decay measurements. Typically measured free decay and strong motion time series, respectively have been shown in figures 3.2 and 3.3. Only strong motion measurements were performed at the last session, since the structure collapsed, see Skjærbæk et al. [1]. Further, it should be noticed that the structure became damaged between the free decay test fd1_b00 and fd1_b01 due to an operation failure of the equipment controlling the shaking table. In table 3.1 references are given to earthquake a, b and c, respectively. These three earthquakes were used throughout the tests for both weak and strong motion excitation of the structure. The earthquake a and b , see figure 3.1, were artificial generated using a white noise sequence filtered through a Kanai-Tajimi filter. Earthquake c, see figure 3.1 was a "real" one measured during the Northridge earthquake on California, USA in 1994.

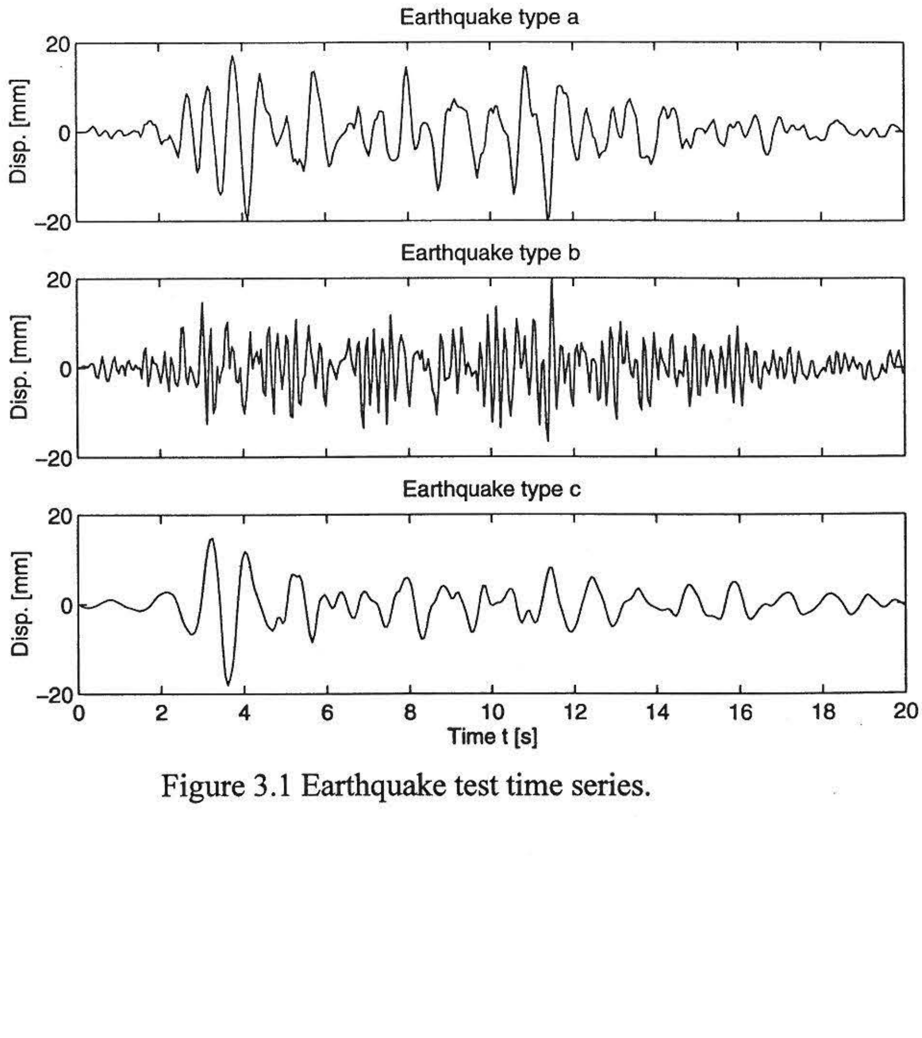

Figure 3.1 Earthquake test time series.

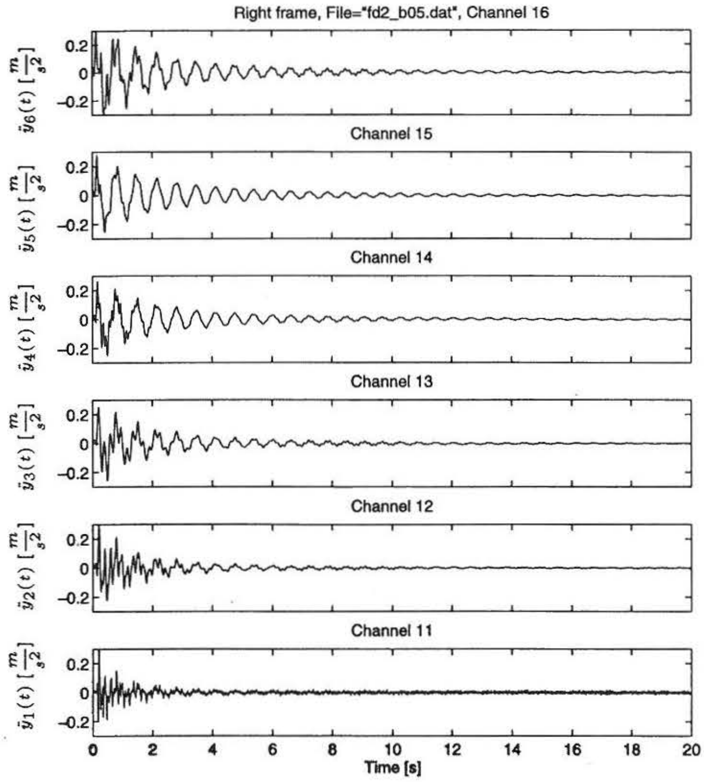

Figure 3.2 Free decay time series.

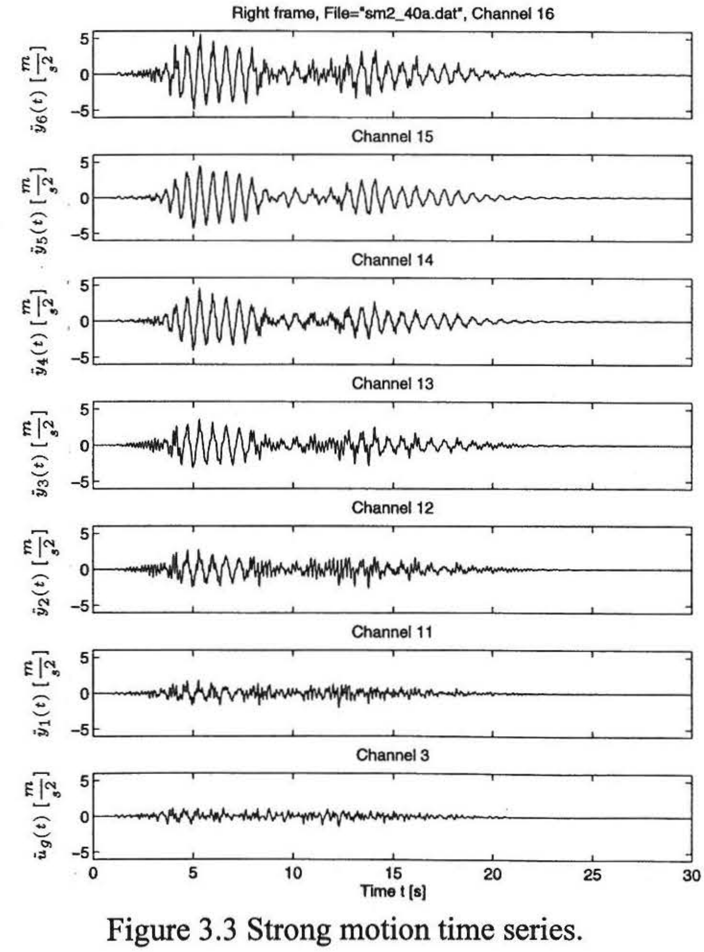

Figure 3.3 Strong motion time series.

3.1.1 Identification and decomposition of bending and rotational modes

Assuming that the structure is symmetrical the accelerometers (15) and (16), respectively will measure responses nearly equal in magnitude for both bending an rotational vibrations and have the same sign in bending out of plane and opposite sign in rotational vibration. Adding signals for the two symmetrical locations doubles the bending response and deletes the rotational response. Subtracting the signals doubles the rotational response and deletes the bending response. Figure 3.4 shows the autospectra of the time series (fd1_r01) obtained from the accelerometers at the locations (15) and (16) . Further, the autospectra obtained by adding and subtracting , (15) and (16), respectively have been shown. From these spectra it is seen that the structure has natural bending frequencies at approximately 2, 7.5 and 9 , respectively. Further, it is seen that natural rotational frequencies exist at approximately 2.5 and 12 Hz., respectively. These conclusions have been used in the following in order to identify the lowest two bending modes in the plane.

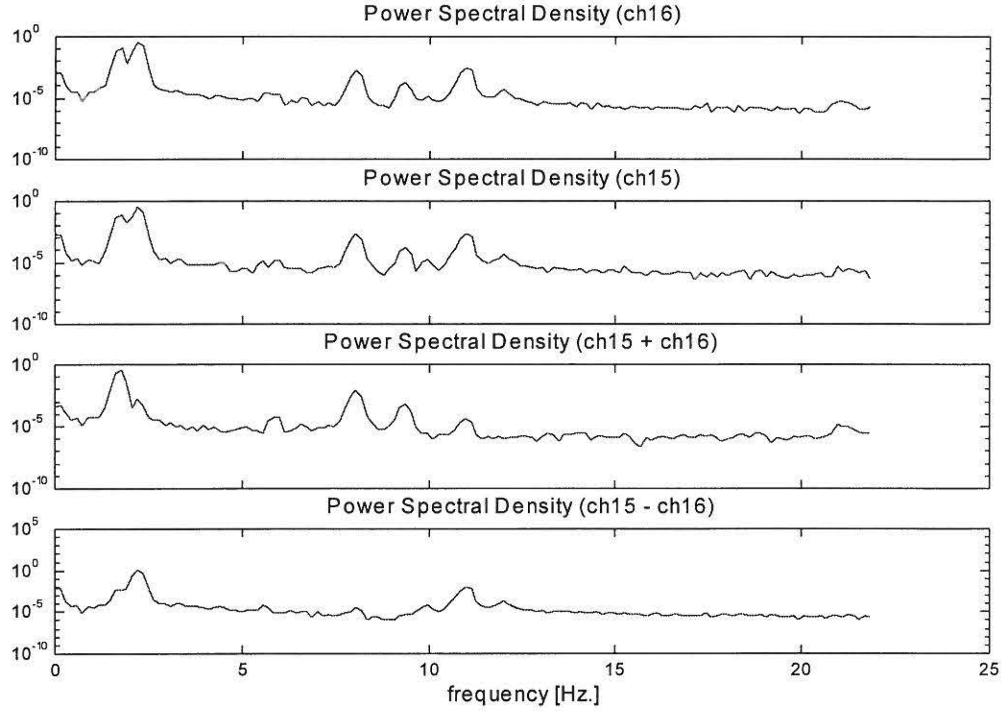

Figure 3.4 Autospectra of the signals from accelerometers at location (15) and (16).

3.2 Analysis of virgin state test data

In the following the results of the system identification using well-proved techniques will be presented. The free-decay time series were analysed by means of the ARV, ERA, Polyreference and ARMAV techniques, see e.g. Pandit [2], Juang [3], Vold [4], Kirkegaard et al. [4]. Results from model selection and validation will not be presented.

SI-method	f_1 [Hz]	f_2 [Hz]	ζ_1 [%]	ζ_2 [%]
ARV	1.929	6.550	2.42	6.37
ERA	1.932	6.538	2.04	2.17
POYLREF	1.925	6.424	2.43	6.77
ARMAV	1.927	6.548	2.59	3.81

Table 3.1 Identified frequencies and damping ratios of the virgin frame structure AAU1(fd1_b00.dat).

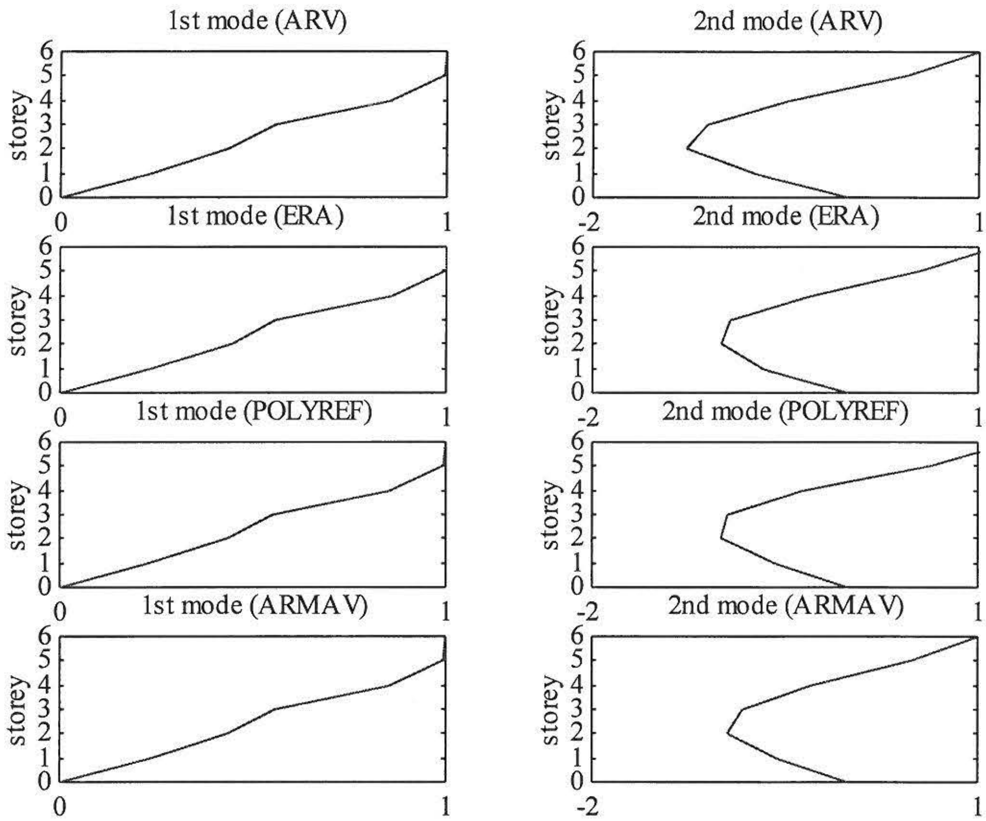

Figure 3.5 Identified mode shapes of the virgin frame structure AAU1 (fd1_b00.dat).

SI-method	f_1 [Hz]	f_2 [Hz]	ζ_1 [%]	ζ_2 [%]
ARV	1.657	5.799	2.62	1.88
ERA	1.653	5.786	2.66	1.60
POYLREF	1.660	5.783	2.22	1.90
ARMAV	1.662	5.788	2.53	2.77

Table 3.2 Identified frequencies and damping ratios of the virgin frame structure AAU1(fd1_b01.dat).

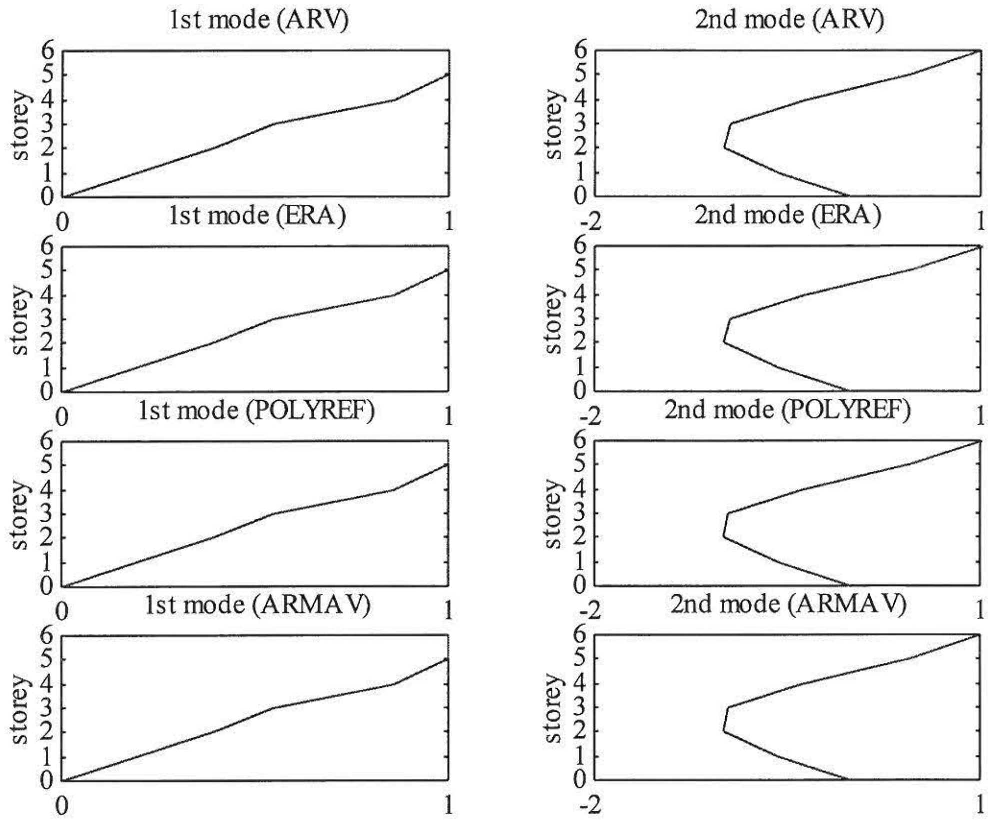

Figure 3.6 Identified mode shapes of the virgin frame structure AAU1 (fd1_b01.dat).

SI-method	f_1 [Hz]	f_2 [Hz]	ζ_1 [%]	ζ_2 [%]
ARV	1.650	5.781	2.72	1.83
ERA	1.652	5.771	2.40	1.71
POYLREF	1.657	5.778	2.52	1.77
ARMAV	1.651	5.789	2.68	1.90

Table 3.3 Identified frequencies and damping ratios of the virgin frame structure AAU1(fd1_b02.dat).

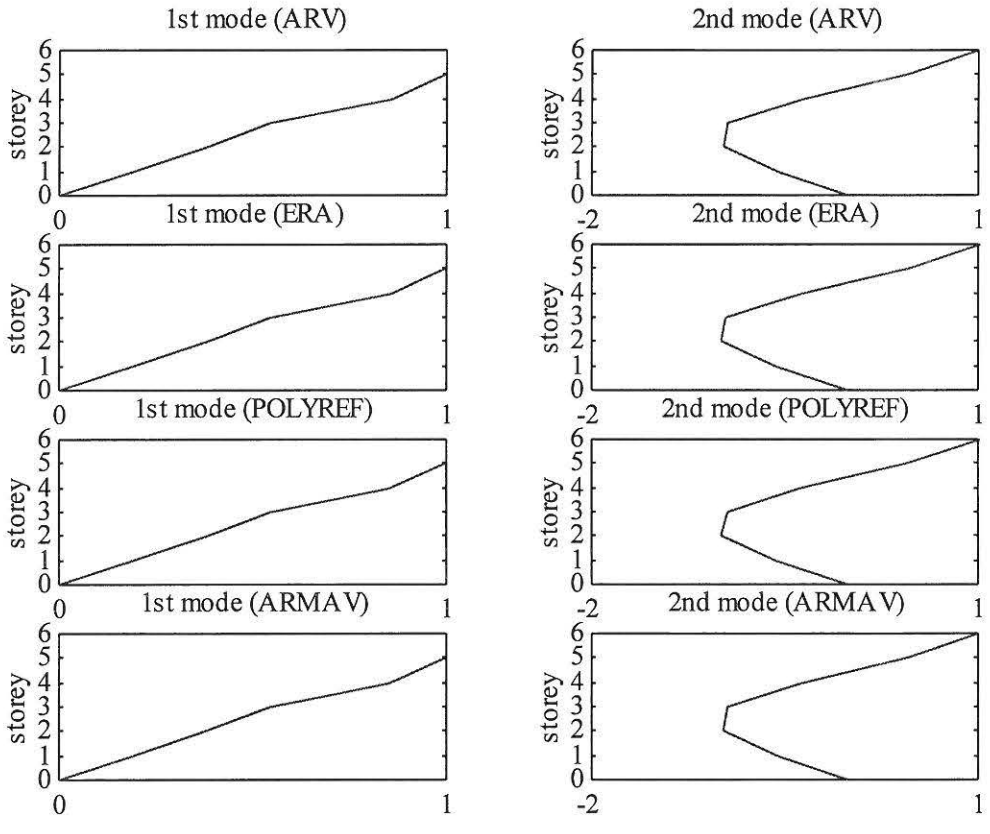

Figure 3.7 Identified mode shapes of the virgin frame structure AAU1 (fd1_b02.dat).

SI-method	f_1 [Hz]	f_2 [Hz]	ζ_1 [%]	ζ_2 [%]
ARV	1.664	5.815	3.37	1.99
ERA	1.662	5.801	2.91	1.67
POYLREF	1.668	5.811	2.77	1.78
ARMAV	1.666	5.817	3.34	2.14

Table 3.4 Identified frequencies and damping ratios of the virgin frame structure-AAU1(fd1_b03.dat)

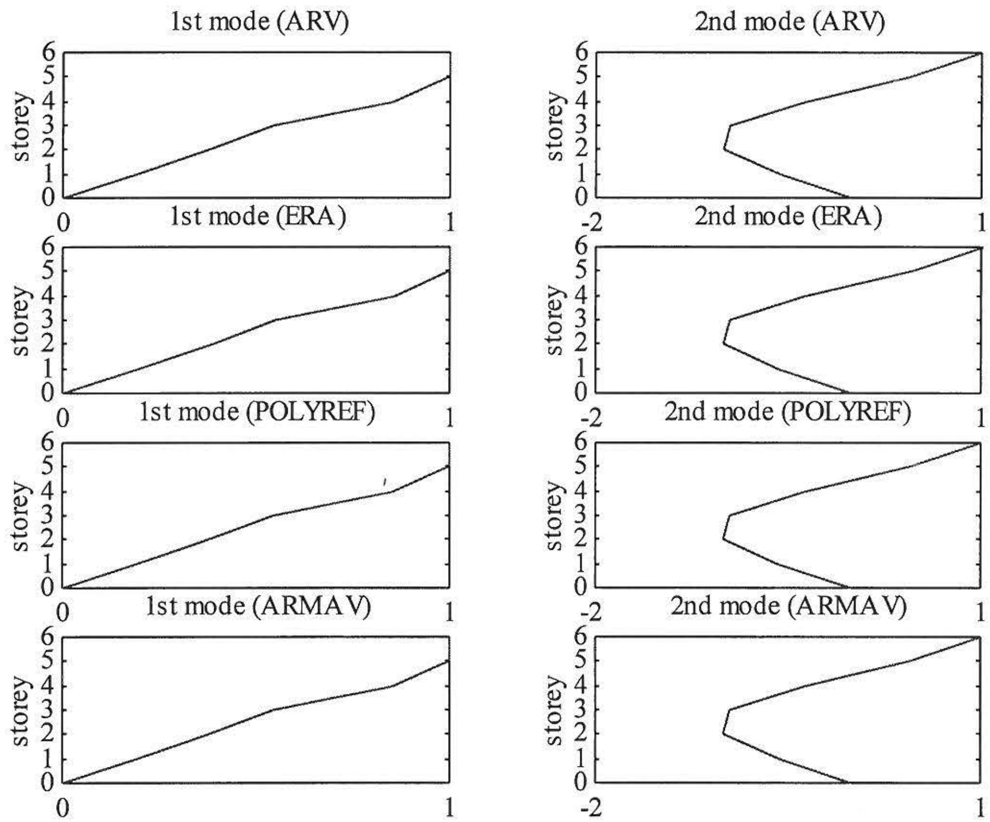

Figure 3.8 Identified mode shapes of the virgin frame structure AAU1 (fd1_b03.dat).

Data	f_1 [Hz]	f_2 [Hz]	ζ_1 [%]	ζ_2 [%]
wm1_ta01.dat	1.706	5.973	2.23	2.31
wm1_tb01.dat	1.713	5.901	2.74	2.08
wm1_tc01.dat	1.701	6.020	2.64	1.35

Table 3.5 Identified frequencies and damping ratios of the virgin frame structure AAU1 from weak motion test data .

3.3 Analysis of test data from the destructive testing

SI-method	f_1 [Hz]	f_2 [Hz]	ζ_1 [%]	ζ_2 [%]
ARV	1.580	5.619	3.80	2.23
ERA	1.571	5.610	3.49	1.96
POYLREF	1.582	5.613	3.39	2.08
ARMAV	1.581	5.643	3.47	2.87

Table 3.6 Identified frequencies and damping ratios of the frame structure AAU1 after EQ1 (fd1_b04.dat).

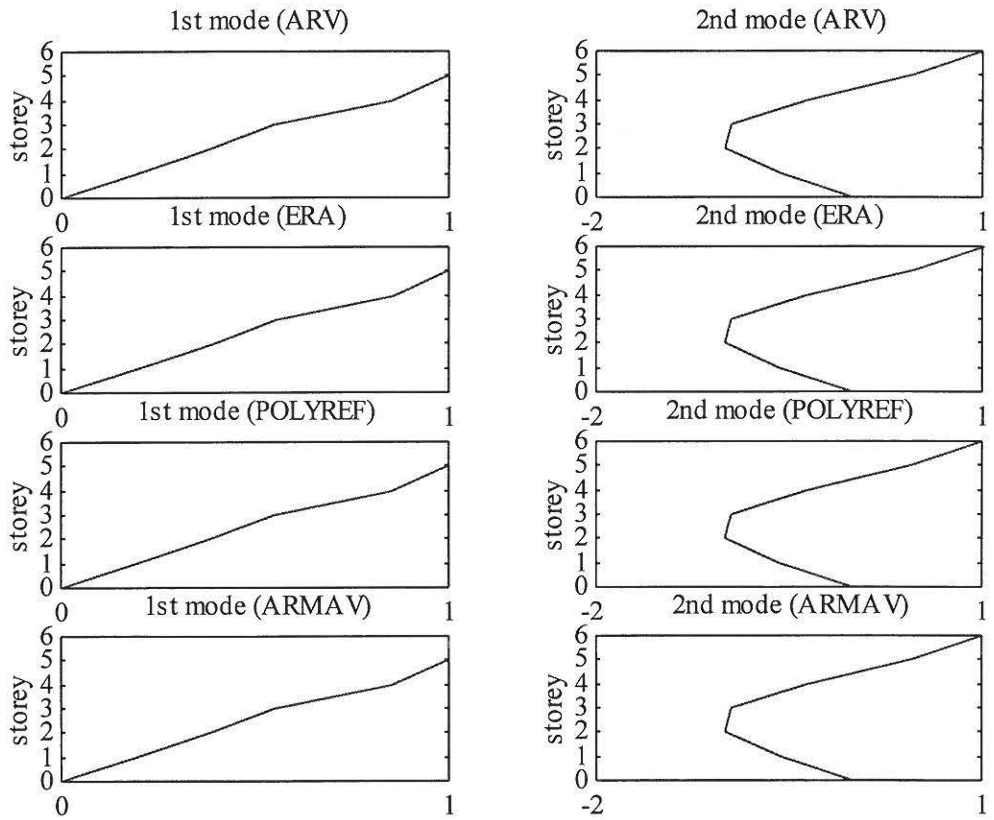

Figure 3.9 Identified mode shapes of the frame structure AAU1 after - EQ1(fd1_b04.dat). [———] : Virgin state, [- - - - -]: damaged structure.

SI-method	f_1 [Hz]	f_2 [Hz]	ζ_1 [%]	ζ_2 [%]
ARV	1.314	5.014	4.41	2.16
ERA	1.311	4.997	4.29	1.78
POYLREF	1.317	5.004	4.32	2.40
ARMAV	1.314	5.015	5.12	2.21

Table 3.7 Identified frequencies and damping ratios of the frame structure AAU1 after EQ2 (fd1_b05.dat).

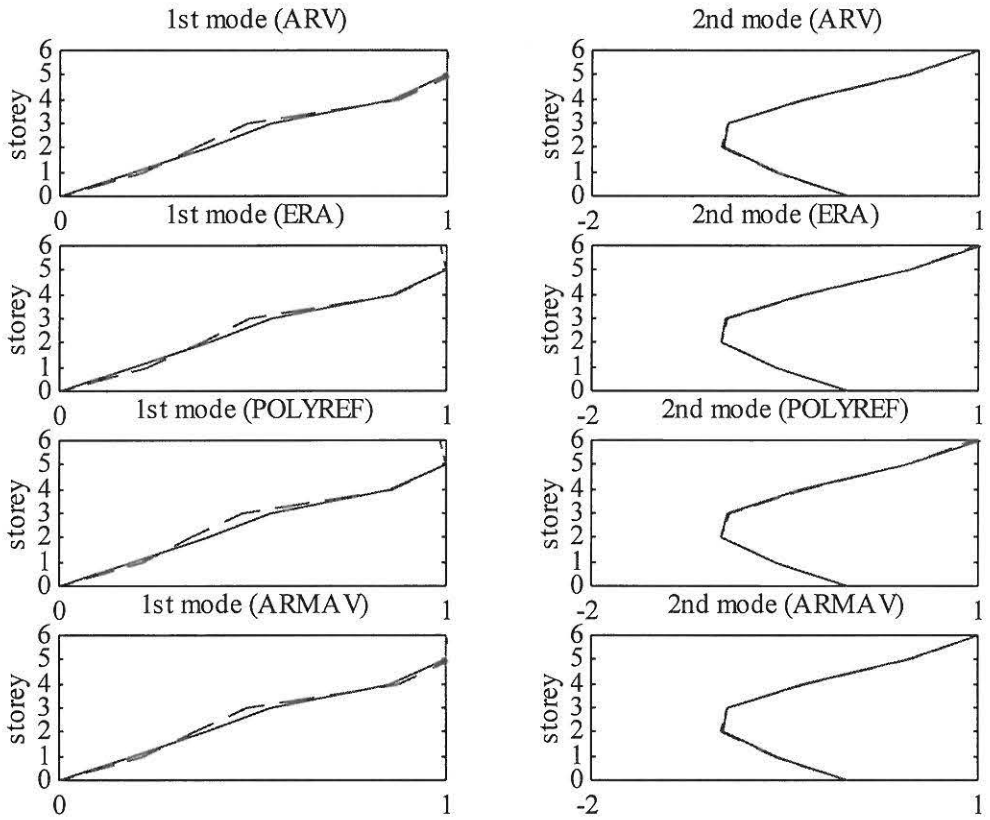

Figure 3.10 Identified mode shapes of the frame structure AAU1 after EQ2 (fd1_b05.dat). [———] : Virgin state, [- - - - -]: damaged structure.

Data	f_1 [Hz]	f_2 [Hz]	ζ_1 [%]	ζ_2 [%]
wm1_1a1.dat	1.629	5.821	1.58	3.43
wm1_1a2.dat	1.436	5.261	2.18	2.23

Table 3.8 Identified frequencies and damping ratios of the frame structure AAU1 from weak motion test data after EQ1 and EQ2, respectively.

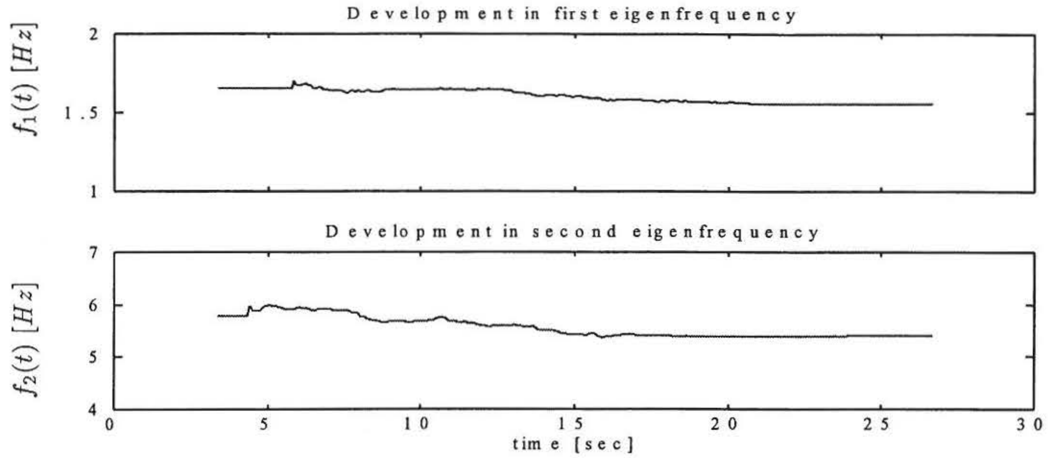

Figure 3.11 Development of softning in first and second mode during EQ1

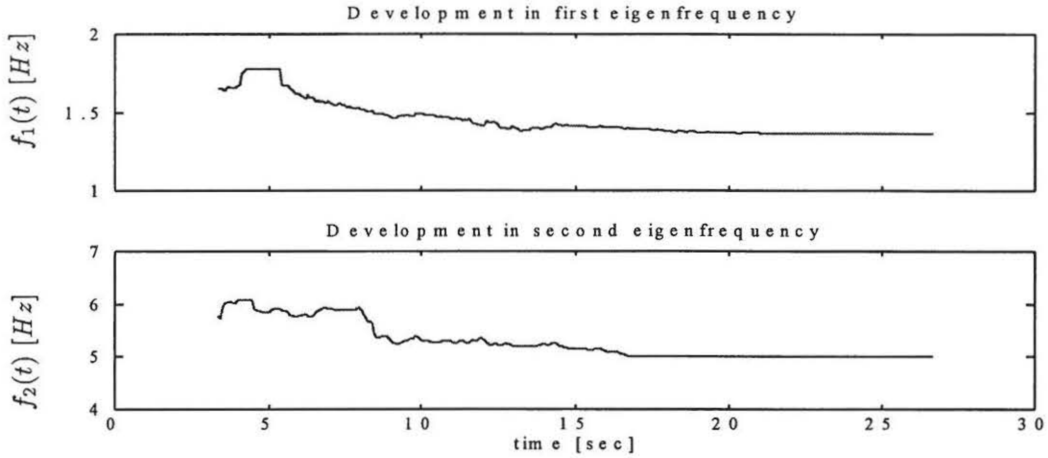

Figure 3.12 Development of softning in first and second mode during EQ2

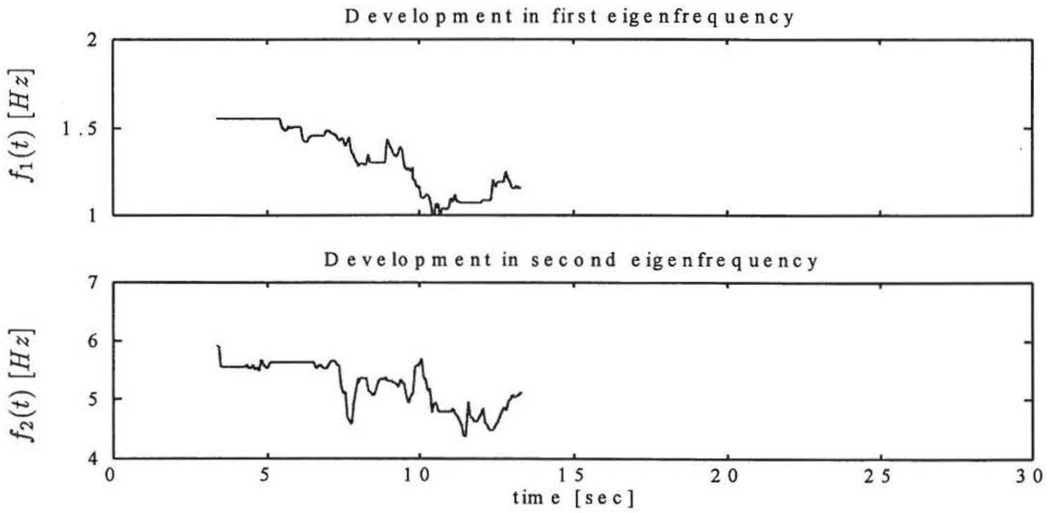

Figure 3.13 Development of softning in first and second mode during EQ3

4 ANALYSIS OF TESTS MEASUREMENTS FROM FRAME AAU2

In this chapter the results from the system identification of frame AAU2 are presented.

4.1 Description of test data from frame AAU2

The files with the data from the performed tests with frame AAU2 are named in table 4.1.

Name	Case
fd2_b01.dat	Free decay in the plane, No. 1. Load = 50 kg
fd2_b02.dat	Free decay in the plane, No. 2. Load = 50 kg
fd2_b03.dat	Free decay in the plane, No. 3. Load = 50 kg
wm2_ta05.dat	Type a earthquake with intensity 1 %
wm2_tb05.dat	Type b earthquake with intensity 1 %
wm2_tc05.dat	Type c earthquake with intensity 1 %
sm2_20a.dat	Strong motion earthquake EQ1 (type a) with intensity of 20 % of max.
wm2_1a1.dat	Weak motion earthquake of type a with intensity 1 % . After EQ1
fd2_b04.dat	Free decay in the plane, No. 4. Load = 50 kg
sm2_40a.dat	Strong motion earthquake EQ2 (type a) with intensity of 40 % of max.
wm2_1a2.dat	Weak motion earthquake of type a with intensity 1 % . After EQ2
fd2_b05.dat	Free decay in the plane, No. 5. Load = 50 kg
fd2_b06.dat	Free decay in the plane, No. 6. Load = 25 kg
fd2_b07.dat	Free decay in the plane, No. 7. Load = 50 kg
fd2_b08.dat	Free decay in the plane, No. 8. Load = 75 kg

Table 4.1 Test data from frame AAU2

From table 4.1 it is seen that 8 free decay measurements, 5 weak motion measurements and 2 strong motion measurements were performed. Three free decay and three weak earthquake tests were performed before the first strong earthquake test in order to make a virgin state identification of the frame. The free-decay tests were performed by means of a excitation set-up implying that the pull-out force could be measured. The following measurement sessions consisted of one strong motion measurement, one weak motion measurement and 1 free decay measurements.
It should be noticed that the frame AAU2 was restricted to move out of the plane after it was found that the frame AAU1 made rotation vibrations during the tests.

4.2 Analysis of virgin state test data

SI-method	f_1 [Hz]	f_2 [Hz]	ζ_1 [%]	ζ_2 [%]
ARV	2.154	6.951	1.43	1.44
ERA	2.140	6.950	1.83	2.17
POYLREF	2.146	6.961	2.09	1.43
ARMAV	2.147	6.961	0.85	1.23

Table 4.2 Identified frequencies and damping ratios of the virgin frame structure AAU2 (fd2_b01.dat). Load = 50 kg.

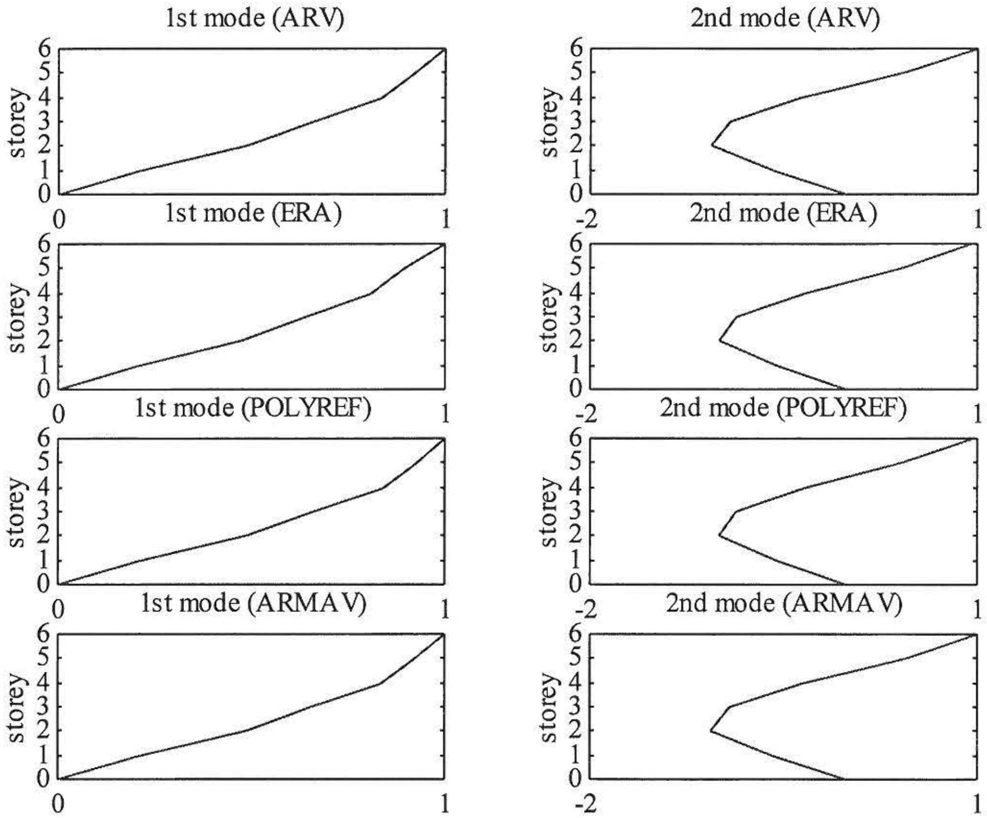

Figure 4.1 Identified mode shapes of the virgin frame structure AAU2 (fd2_b01.dat). Load =50 kg.

SI-method	f_1 [Hz]	f_2 [Hz]	ζ_1 [%]	ζ_2 [%]
ARV	2.147	6.948	1.70	1.37
ERA	2.139	6.943	1.76	1.40
POYLREF	2.148	6.950	1.70	1.39
ARMAV	2.137	6.948	1.70	1.50

Table 4.3 Identified frequencies and damping ratios of the virgin frame structure AAU2 (fd2_b02.dat). Load =50 kg.

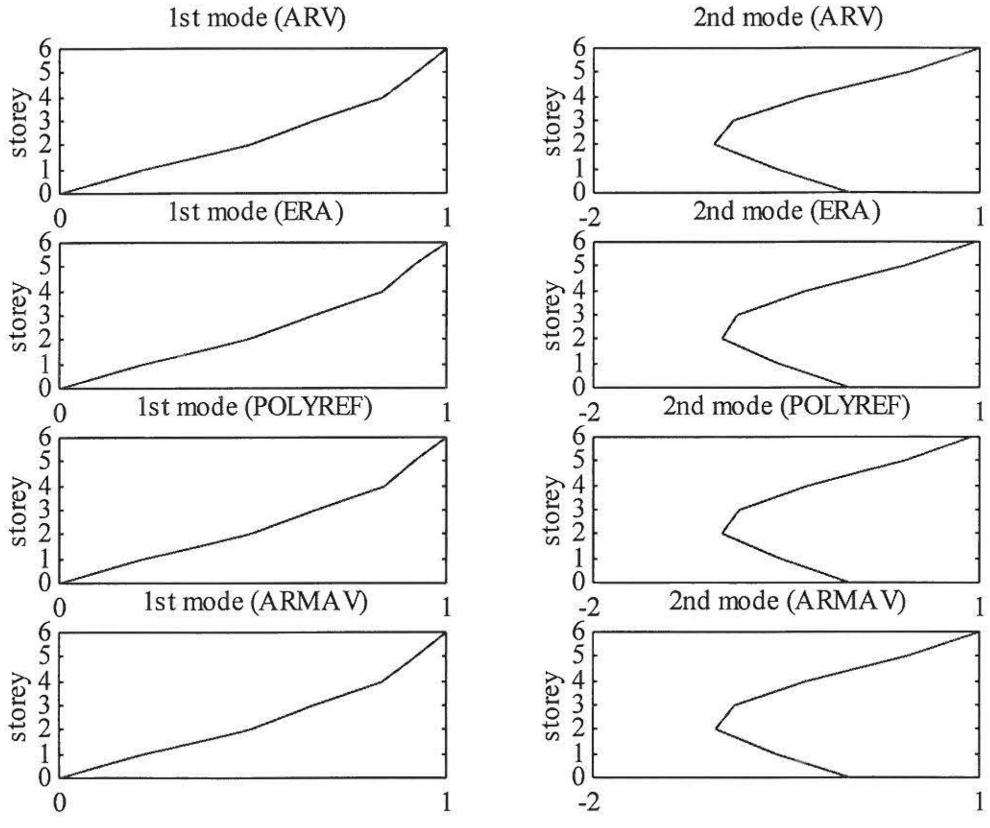

Figure 4.2 Identified mode shapes of the virgin frame structure AAU2 (fd2_b02.dat). Load =50 kg.

SI-method	f_1 [Hz]	f_2 [Hz]	ζ_1 [%]	ζ_2 [%]
ARV	2.149	6.950	1.80	1.41
ERA	2.141	6.945	1.80	1.37
POYLREF	2.149	6.952	1.69	1.31
ARMAV	2.147	6.952	1.74	1.32

Table 4.4 Identified frequencies and damping ratios of the virgin frame structure AAU2 (fd2_b03.dat). Load = 50 kg.

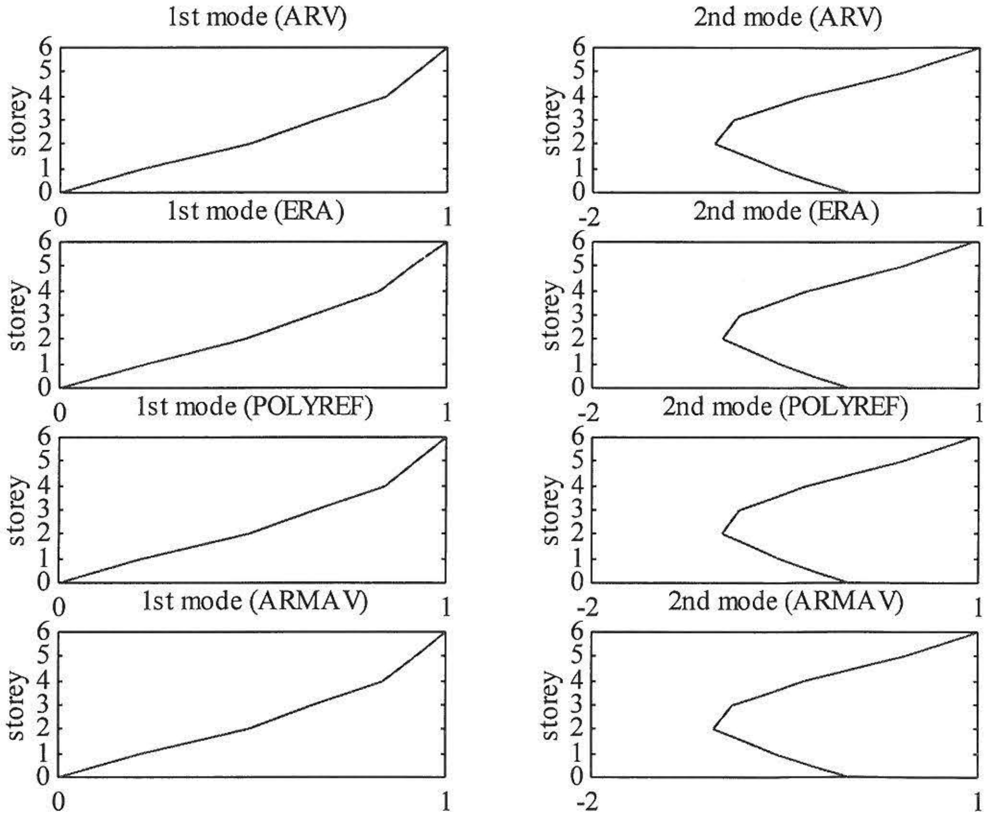

Figure 4.3 Identified mode shapes of the virgin frame structure AAU2 (fd2_b03.dat). Load = 50 kg.

Data	f_1 [Hz]	f_2 [Hz]	ζ_1 [%]	ζ_2 [%]
wm2_ta01.dat	2.211	7.221	1.81	2.64
wm2_tb01.dat	2.217	7.131	1.78	2.02
wm2_tc01.dat	2.211	7.189	1.51	2.66

Table 4.5 Identified frequencies and damping ratios of the virgin frame structure AAU2 from weak motion test data.

4.3 Analysis of test data from the destructive testing

SI-method	f_1 [Hz]	f_2 [Hz]	ζ_1 [%]	ζ_2 [%]
ARV	1.791	6.133	2.86	2.52
ERA	1.771	6.143	3.22	2.80
POYLREF	1.783	6.149	3.27	2.44
ARMAV	1.797	6.093	1.69	2.67

Table 4.6 Identified frequencies and damping ratios of the frame structure AAU2 after EQ1 (fd2_b04.dat). Load = 50 kg.

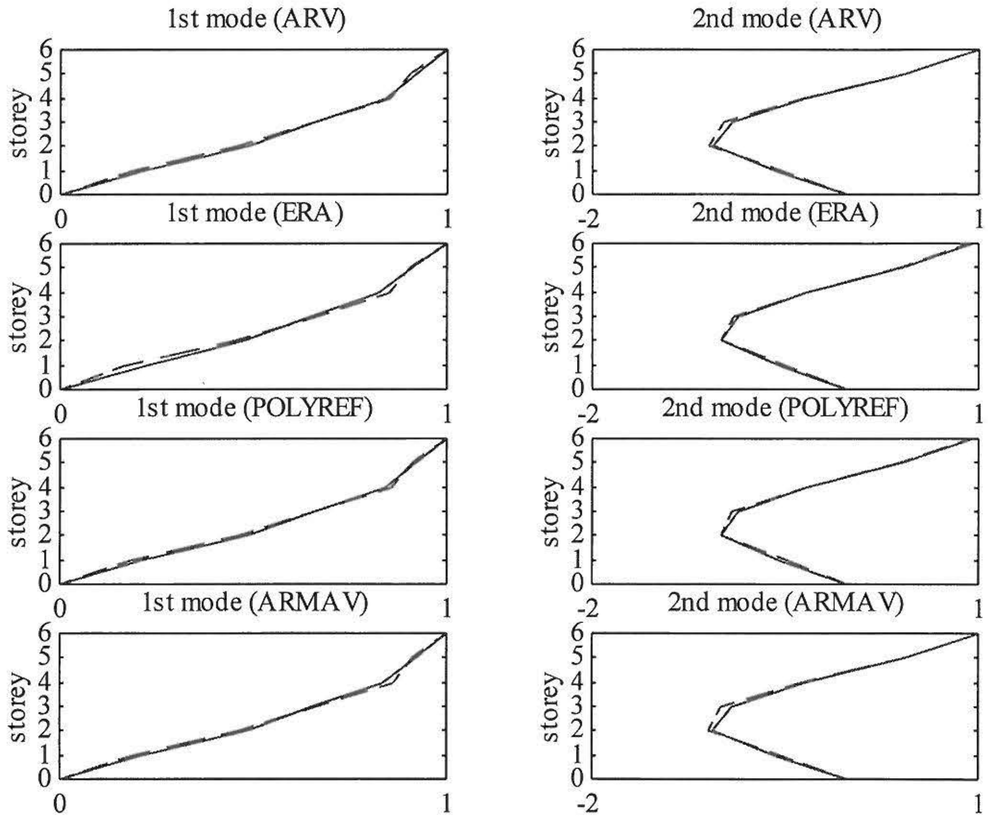

Figure 4.4 Identified mode shapes of the frame structure AAU2 after EQ1 (fd2_b04.dat). Load = 50 kg. [————] : Virgin state, [- - - - -]: damaged structure.

SI-method	f_1 [Hz]	f_2 [Hz]	ζ_1 [%]	ζ_2 [%]
ARV	1.476	5.379	3.83	2.88
ERA	1.463	5.365	3.71	2.65
POYLREF	1.477	5.376	4.17	2.69
ARMAV	1.463	5.369	3.36	2.85

Table 4.7 Identified frequencies and damping ratios of the frame structure AAU2 after EQ2 (fd2_b05.dat). Load = 50 kg.

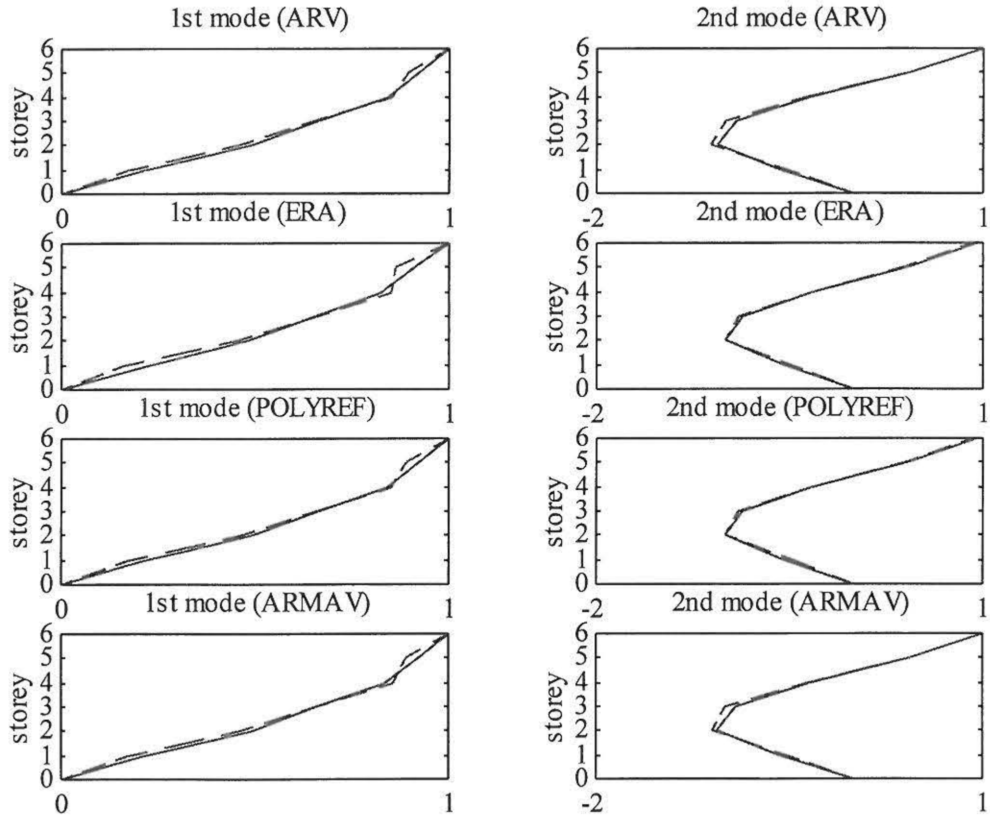

Figure 4.5 Identified mode shapes of the frame structure AAU2 after EQ2 (fd2_b05.dat). Load = 50 kg. [———] : Virgin state, [- - - - -]: damaged structure.

SI-method	f_1 [Hz]	f_2 [Hz]	ζ_1 [%]	ζ_2 [%]
ARV	1.575	5.619	2.74	2.16
ERA	1.564	5.631	3.30	2.05
POYLREF	1.577	5.638	3.17	1.96
ARMAV	1.588	5.621	2.32	1.93

Table 4.8 Identified frequencies and damping ratios of the frame structure AAU2 after EQ2 (fd2_b06.dat). Load = 25 kg.

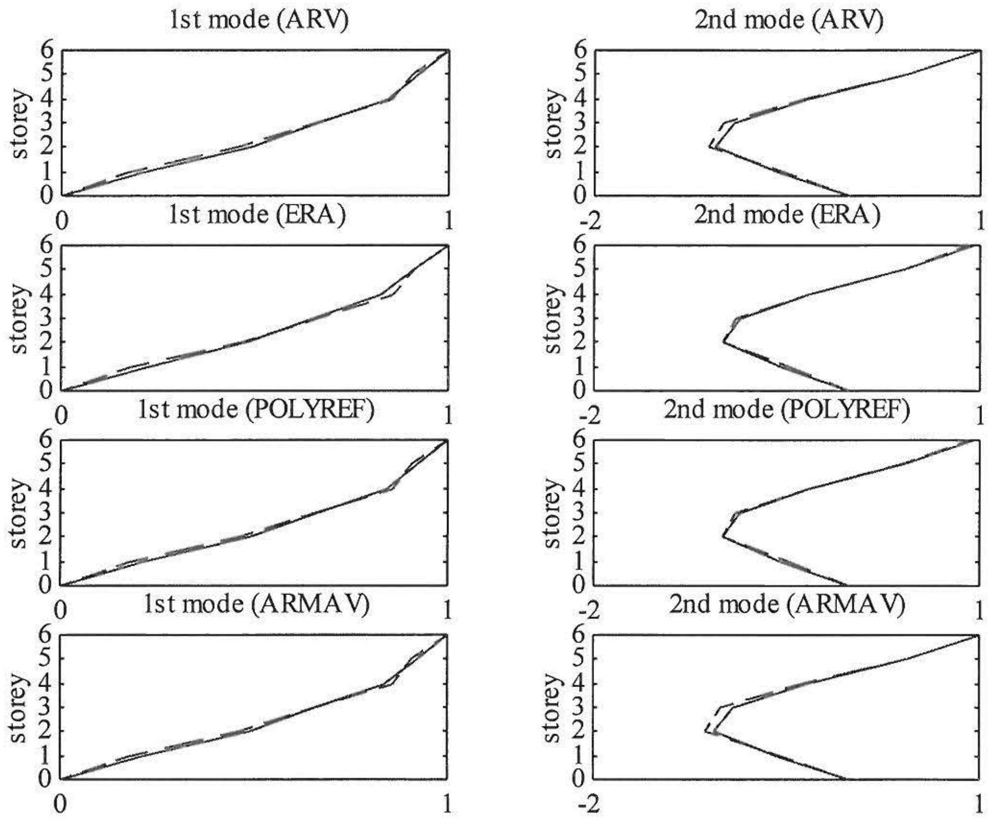

Figure 4.6 Identified mode shapes of the frame structure AAU2 after EQ2 (fd2_b06.dat).Load = 25 kg. [———] : Virgin state, [- - - - -]: damaged structure.

SI-method	f_1 [Hz]	f_2 [Hz]	ζ_1 [%]	ζ_2 [%]
ARV	1.502	5.431	3.42	2.80
ERA	1.489	5.427	3.44	2.49
POYLREF	1.504	5.447	4.17	2.61
ARMAV	1.509	5.443	3.13	2.77

Table 4.9 Identified frequencies and damping ratios of the frame structure AAU2 after EQ2 (fd2_b07.dat). Load = 50 kg.

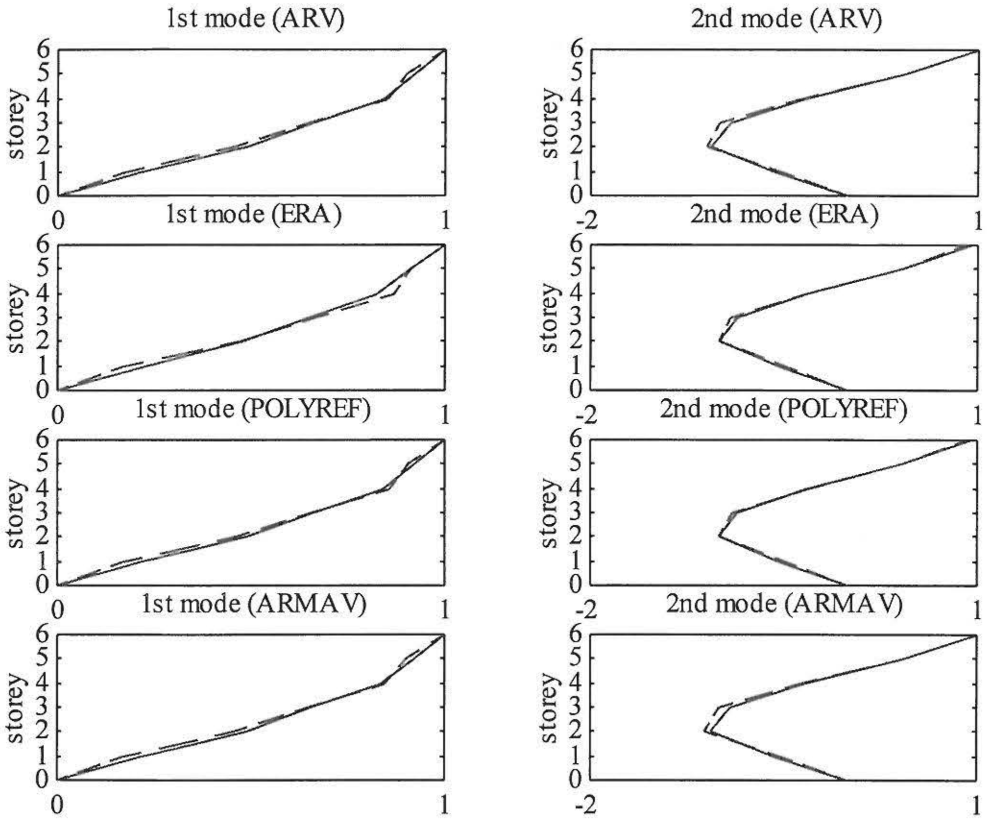

Figure 4.7 Identified mode shapes of the frame structure AAU2 after EQ2 (fd2_b07.dat). Load = 50 kg. [———] : Virgin state, [- - - - -]: damaged structure.

SI-method	f_1 [Hz]	f_2 [Hz]	ζ_1 [%]	ζ_2 [%]
ARV	1.477	5.346	3.86	3.11
ERA	1.453	5.339	3.54	2.80
POYLREF	1.480	5.362	3.27	2.80
ARMAV	1.481	5.322	3.74	2.83

Table 4.10 Identified frequencies and damping ratios of the frame structure AAU2 after EQ2 (fd2_b08.dat). Load = 75 kg.

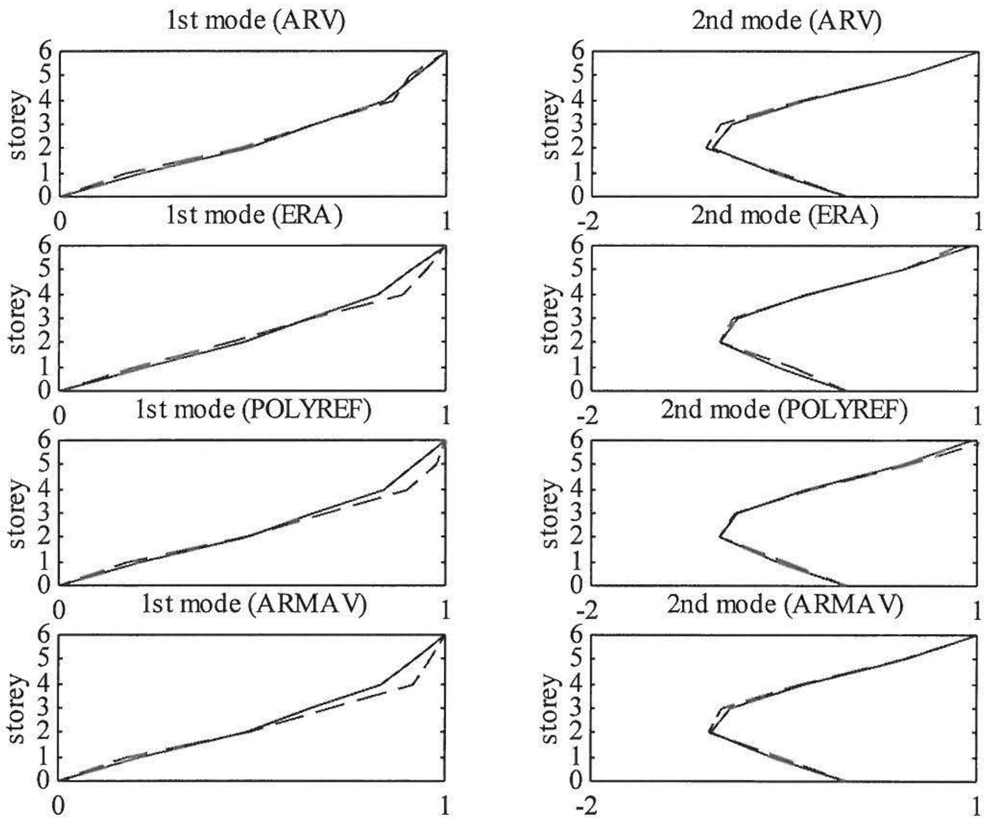

Figure 4.8 Identified mode shapes of the frame structure AAU2 after EQ2 (fd2_b08.dat). Load = 50 kg. [———] : Virgin state, [- - - - -]: damaged structure.

Data	f_1 [Hz]	f_2 [Hz]	ζ_1 [%]	ζ_2 [%]
wm2_1a1.dat	1.877	6.449	1.05	1.66
wm2_1a2.dat	1.609	5.698	1.07	1.53

Table 4.11 Identified frequencies and damping ratios of the frame structure AAU2 from weak motion test data .

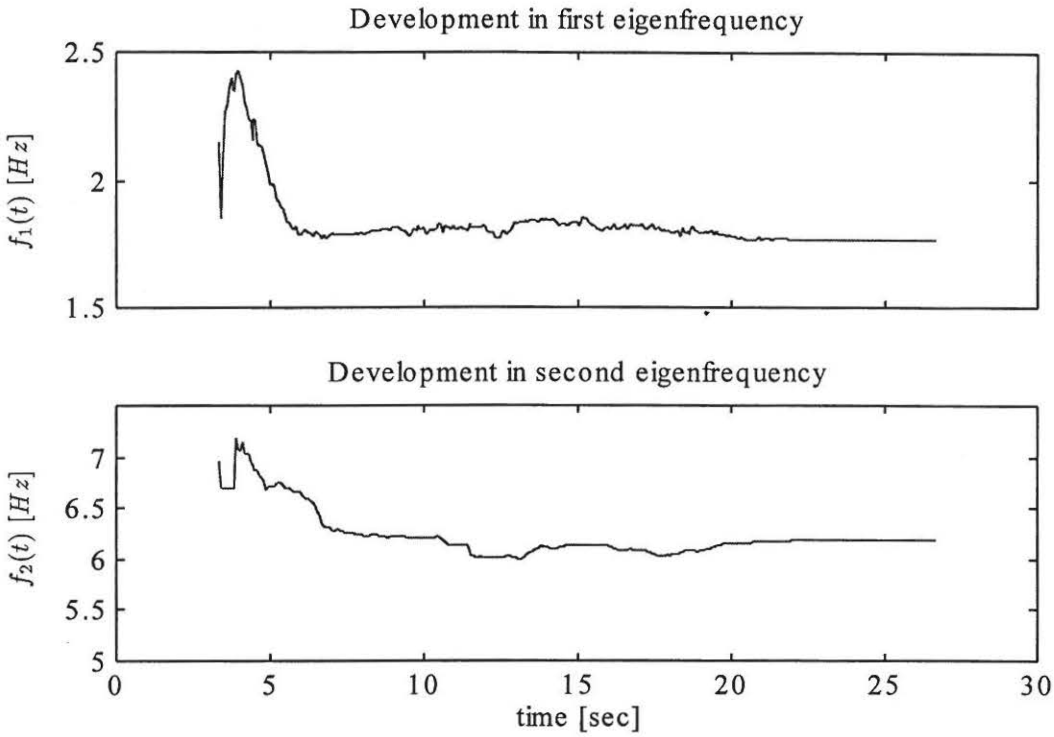

Figure 4.9 Development of softning in first and second mode during EQ1for AAU2.

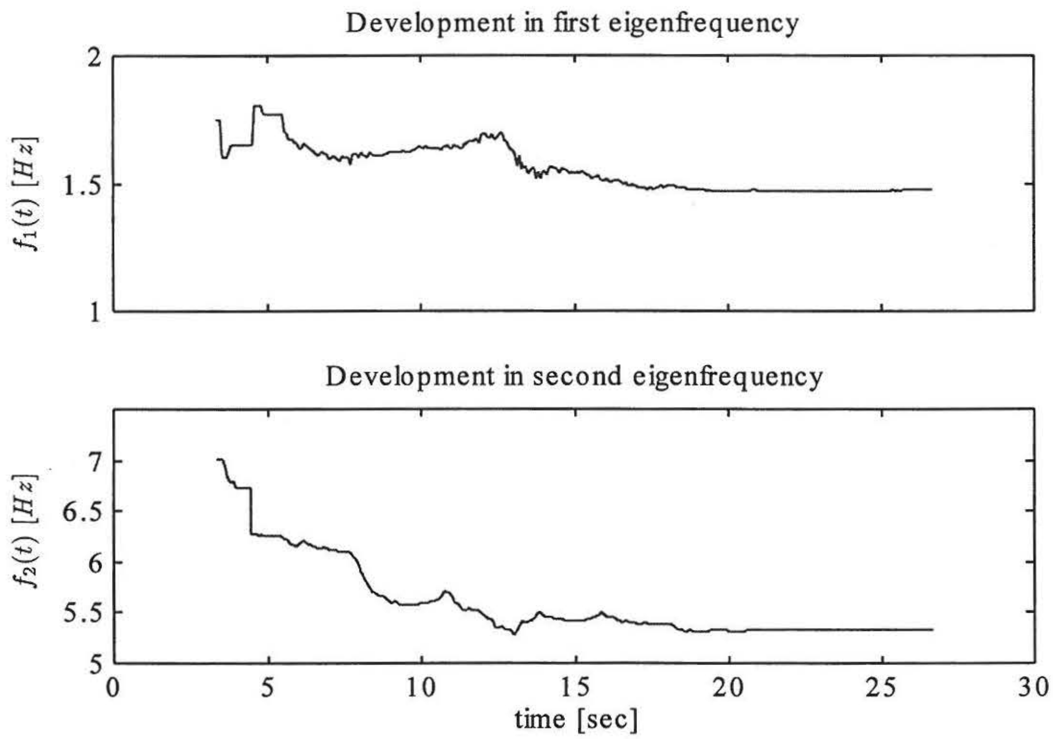

Figure 4.10 Development of softning in first and second mode during EQ2 for AAU2.

5 ANALYSIS OF TESTS MEASUREMENTS FROM FRAME AAU3

In this chapter the results from the system identification of frame AAU3 are presented.

5.1 Description of test data from frame AAU3

The files with the data from the performed tests with frame AAU3 are named in table 5.1.

Name	Case
fd3_b01.dat	Free decay in the plane, Load = 50 kg
fd3_b02.dat	Free decay in the plane, Load = 50 kg
fd3_b03.dat	Free decay in the plane, Load = 50 kg
fd3_b04.dat	Free decay in the plane, Load = 25 kg
fd3_b05.dat	Free decay in the plane, Load = 75 kg
sm3_10a.dat	Strong motion earthquake EQ1 (type b) with intensity 10 % of max.
fd3_b06.dat	Free decay in the plane, Load = 25 kg
fd3_b07.dat	Free decay in the plane, Load = 50 kg
fd3_b08.dat	Free decay in the plane, Load = 75 kg (file damaged)
sm3_20a.dat	Strong motion earthquake EQ2 (type b) with intensity 20 % of max.
fd3_b09.dat	Free decay in the plane, Load = 25 kg
fd3_b10.dat	Free decay in the plane, Load = 50 kg
fd3_b11.dat	Free decay in the plane, Load = 75 kg
sm3_35a.dat	Strong motion earthquake EQ3 (type b) with intensity 35 % of max.
fd3_b12.dat	Free decay in the plane, Load = 25 kg (file damaged)
fd3_b13.dat	Free decay in the plane, Load = 50 kg
fd3_b14.dat	Free decay in the plane, Load = 75 kg

Table 5.1 Test data from frame AAU3.

From table 5.1 it is seen that 14 free decay measurements and 3 strong motion measurements were performed. It should be noticed that the frame AAU3 was restricted to move in the plane as frame AAU2. Further, frame AAU3 was not tested by weak earthquake motion.

5.2 Analysis of virgin state test data

SI-method	f_1 [Hz]	f_2 [Hz]	ζ_1 [%]	ζ_2 [%]
ARV	2.251	7.284	1.49	0.96
ERA	2.246	7.280	1.47	0.98
POYLREF	2.253	7.291	1.41	0.96
ARMAV	2.251	7.287	1.40	1.00

Table 5.2 Identified frequencies and damping ratios of the virgin frame structure AAU3 (fd3_b01.dat). Load = 50 kg.

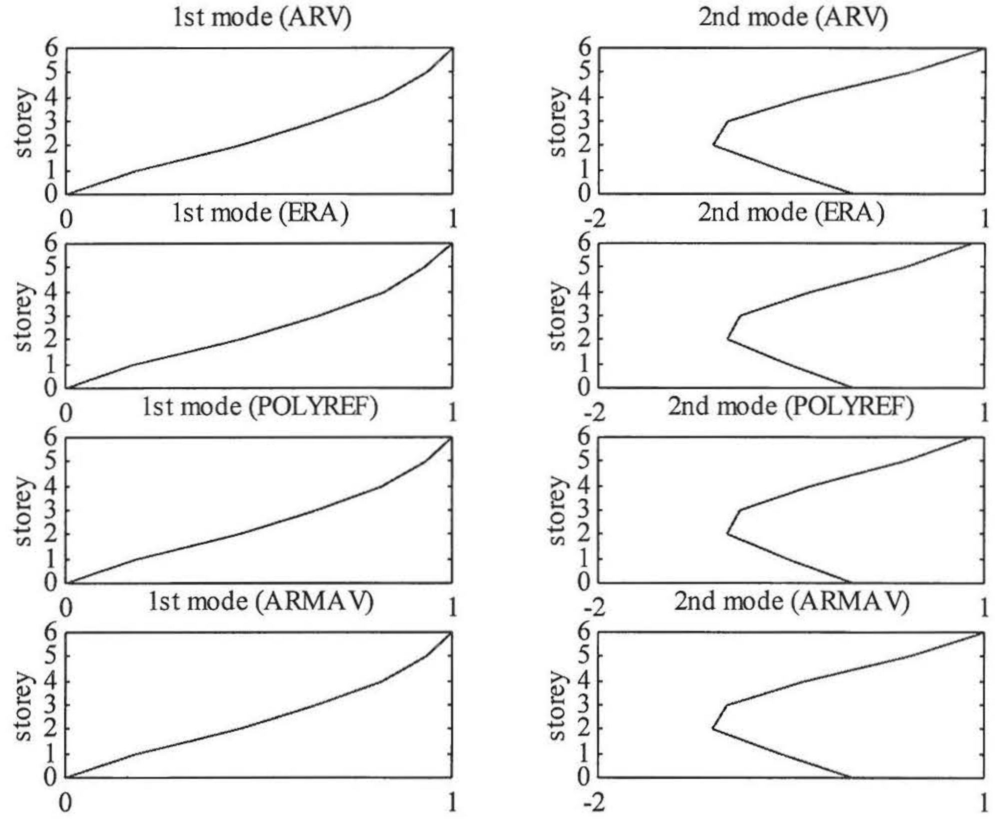

Figure 5.1 Identified mode shapes of the virgin frame structure AAU3 (fd3_b01.dat). Load = 50 kg.

SI-method	f_1 [Hz]	f_2 [Hz]	ζ_1 [%]	ζ_2 [%]
ARV	2.248	7.274	1.46	0.97
ERA	2.243	7.271	1.46	0.95
POYLREF	2.249	7.281	1.40	0.96
ARMAV	2.248	7.273	1.48	0.89

Table 5.3 Identified frequencies and damping ratios of the virgin frame structure AAU3 (fd3_b02.dat). Load =50 kg.

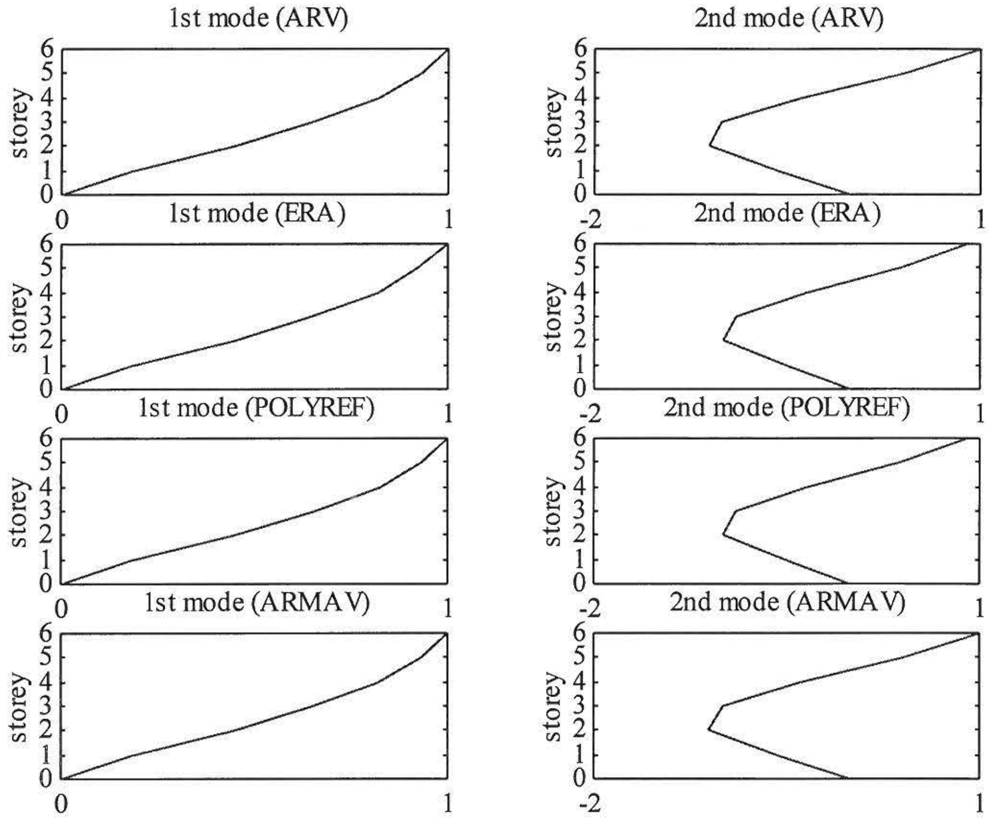

Figure 5.2 Identified mode shapes of the virgin frame structure AAU3 (fd3_b02.dat). Load =50 kg.

SI-method	f_1 [Hz]	f_2 [Hz]	ζ_1 [%]	ζ_2 [%]
ARV	2.244	7.264	1.44	0.94
ERA	2.239	7.261	1.46	0.97
POYLREF	2.244	7.270	1.40	0.96
ARMAV	2.244	7.262	1.60	0.94

Table 5.4 Identified frequencies and damping ratios of the virgin frame structure AAU3. (fd3_b03.dat). Load = 50 kg.

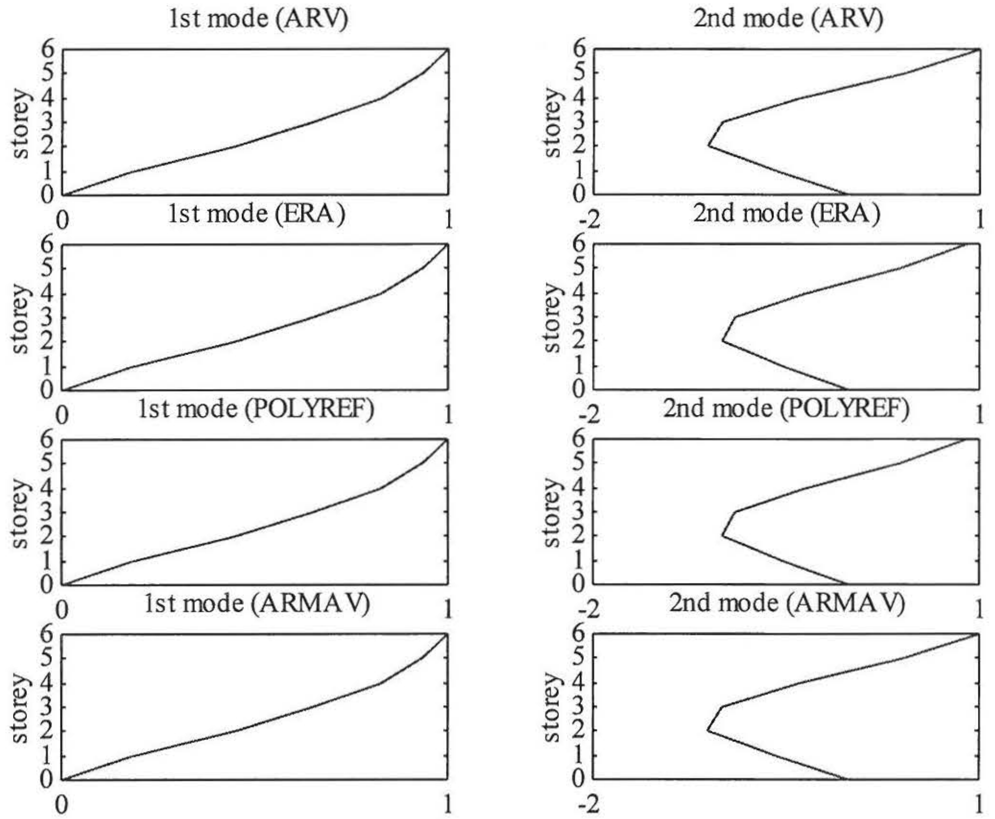

Figure 5.3 Identified mode shapes of the virgin frame structure AAU3 (fd3_b03.dat). Load = 50 kg.

SI-method	f_1 [Hz]	f_2 [Hz]	ζ_1 [%]	ζ_2 [%]
ARV	2.197	7.149	1.70	1.13
ERA	2.190	7.145	1.75	1.14
POYLREF	2.197	7.155	1.68	1.16
ARMAV	2.196	7.146	1.61	1.11

Table 5.5 Identified frequencies and damping ratios of the virgin frame structure AAU3 (fd3_b04.dat). Load = 25 kg.

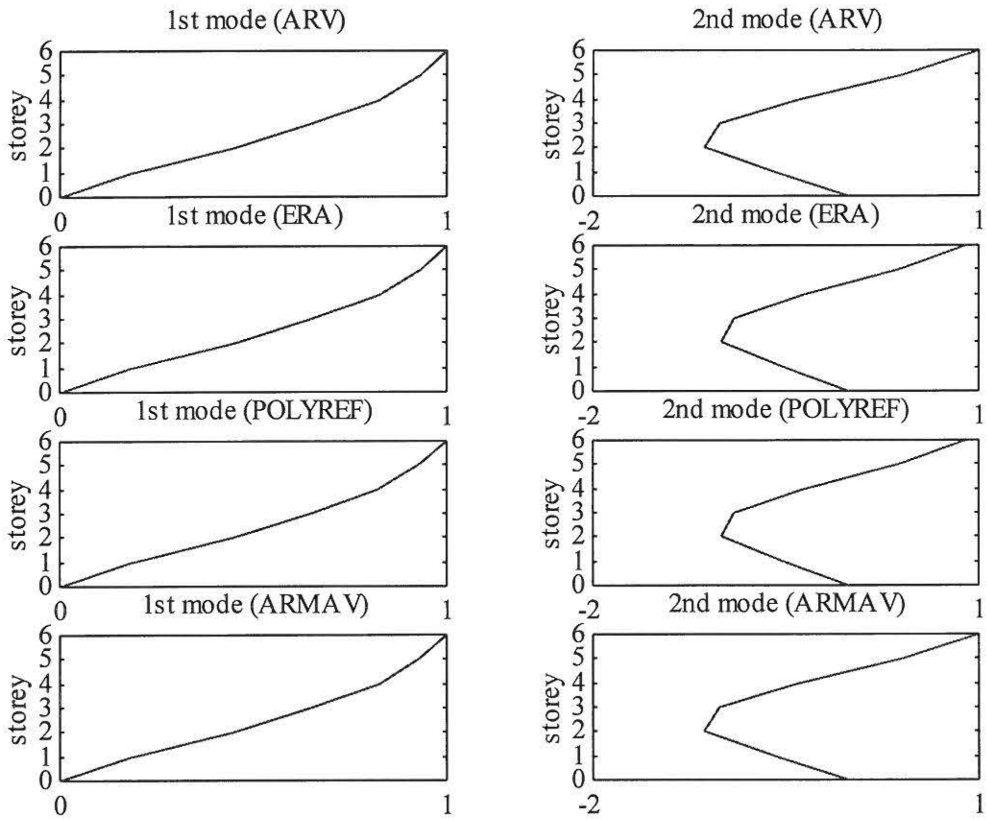

Figure 5.4 Identified mode shapes of the virgin frame structure AAU3 (fd3_b04.dat). Load = 25 kg

SI-method	f_1 [Hz]	f_2 [Hz]	ζ_1 [%]	ζ_2 [%]
ARV	2.252	7.289	1.41	0.93
ERA	2.247	7.278	1.40	0.90
POYLREF	2.253	7.292	1.37	0.93
ARMAV	2.249	7.285	1.47	0.98

Table 5.6 Identified frequencies and damping ratios of the virgin frame structure AAU3 (fd3_b05.dat). Load = 75 kg.

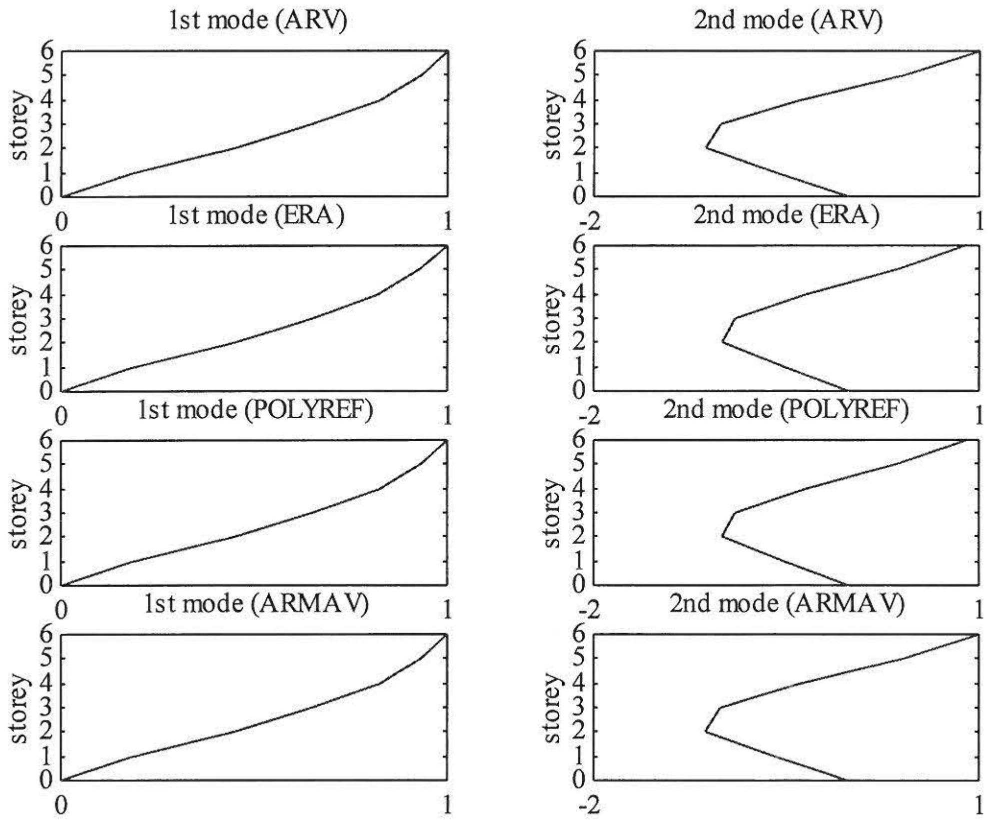

Figure 5.5 Identified mode shapes of the vigin frame structure AAU3 (fd3_b05.dat). Load = 50 kg.

5.3 Analysis of test data from the destructive testing

SI-method	f_1 [Hz]	f_2 [Hz]	ζ_1 [%]	ζ_2 [%]
ARV	2.031	6.545	2.05	1.40
ERA	2.022	6.540	2.15	1.23
POYLREF	2.034	6.558	1.98	1.32
ARMAV	2.029	6.537	2.11	1.64

Table 5.7 Identified frequencies and damping ratios of the frame structure AAU3 after EQ1 (fd3_b06.dat). Load = 25 kg.

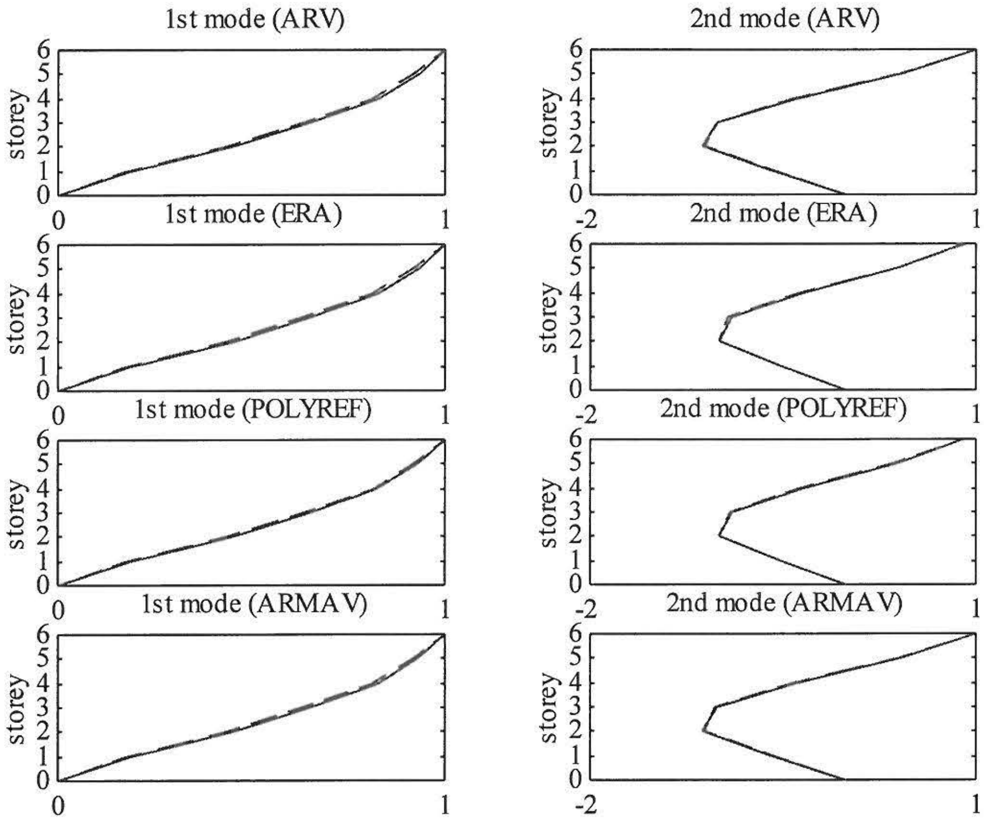

Figure 5.6 Identified mode shapes of the frame structure AAU3 after EQ1 (fd3_b06.dat). Load = 25 kg. [———] : Virgin state, [- - - - -]: damaged structure.

SI-method	f_1 [Hz]	f_2 [Hz]	ζ_1 [%]	ζ_2 [%]
ARV	1.798	5.858	2.88	2.12
ERA	1.789	5.832	2.96	1.92
POYLREF	1.792	5.837	2.59	1.95
ARMAV	1.798	5.847	3.02	1.96

Table 5.9 Identified frequencies and damping ratios of the frame structure AAU3 after EQ2 (fd3_b09.dat). Load = 25 kg.

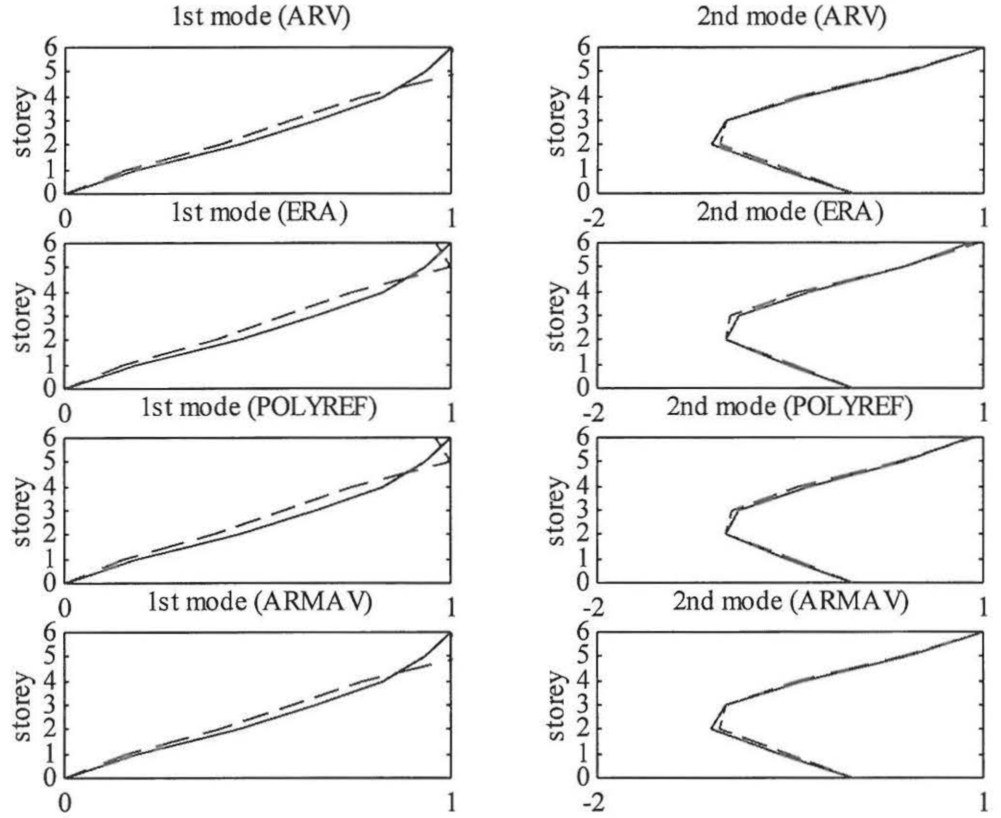

Figure 5.8 Identified mode shapes of the frame structure after EQ2 AAU3 (fd3_b09.dat). Load = 25 kg. [――――] : Virgin state, [- - - - -]: damaged structure.

SI-method	f_1 [Hz]	f_2 [Hz]	ζ_1 [%]	ζ_2 [%]
ARV	1.733	5.679	3.19	2.40
ERA	1.722	5.651	3.26	1.93
POYLREF	1.734	5.655	3.19	1.97
ARMAV	1.736	5.682	3.46	2.31

Table 5.10 Identified frequencies and damping ratios of the frame structure AAU3 after EQ2 (fd3_b10.dat). Load =50 kg.

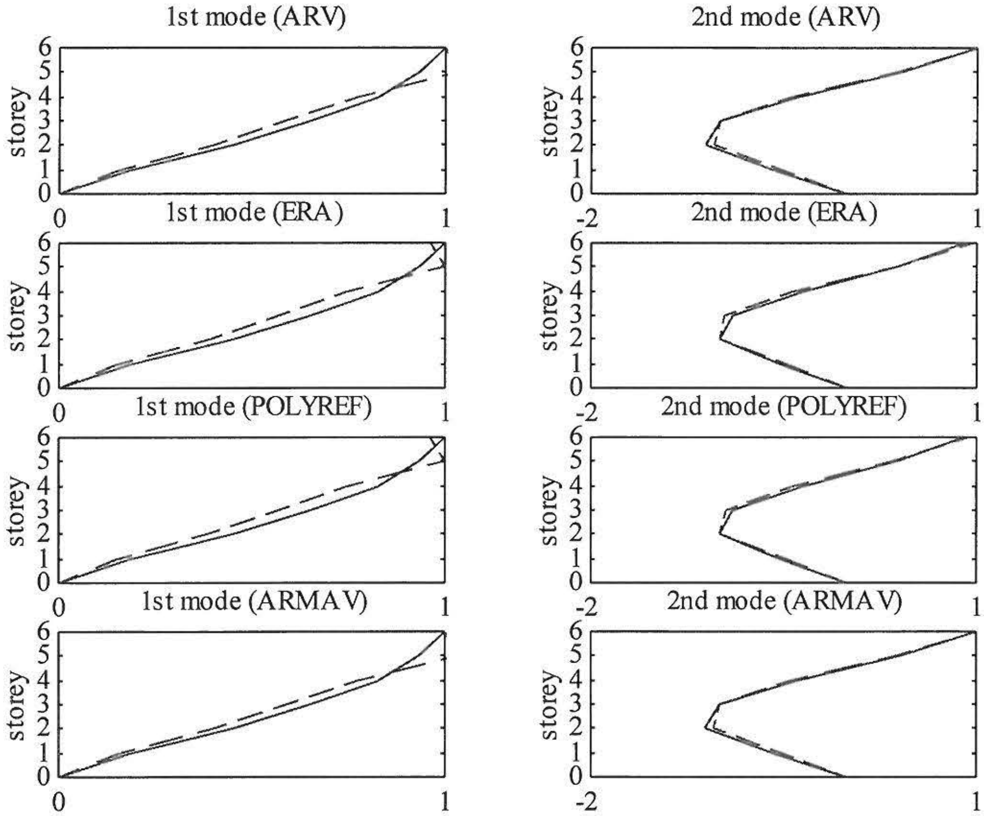

Figure 5.9 Identified mode shapes of the frame structure after EQ2 AAU3 (fd3_b10.dat). Load = 50 kg. [————] : Virgin state, [- - - - -]: damaged structure.

SI-method	f_1 [Hz]	f_2 [Hz]	ζ_1 [%]	ζ_2 [%]
ARV	1.696	5.556	3.54	2.65
ERA	1.680	5.541	3.29	2.08
POYLREF	1.691	5.557	3.22	2.05
ARMAV	1.693	5.556	3.97	2.82

Table 5.11 Identified frequencies and damping ratios of the frame structure AAU3 after EQ2 (fd3_b11.dat). Load = 75 kg.

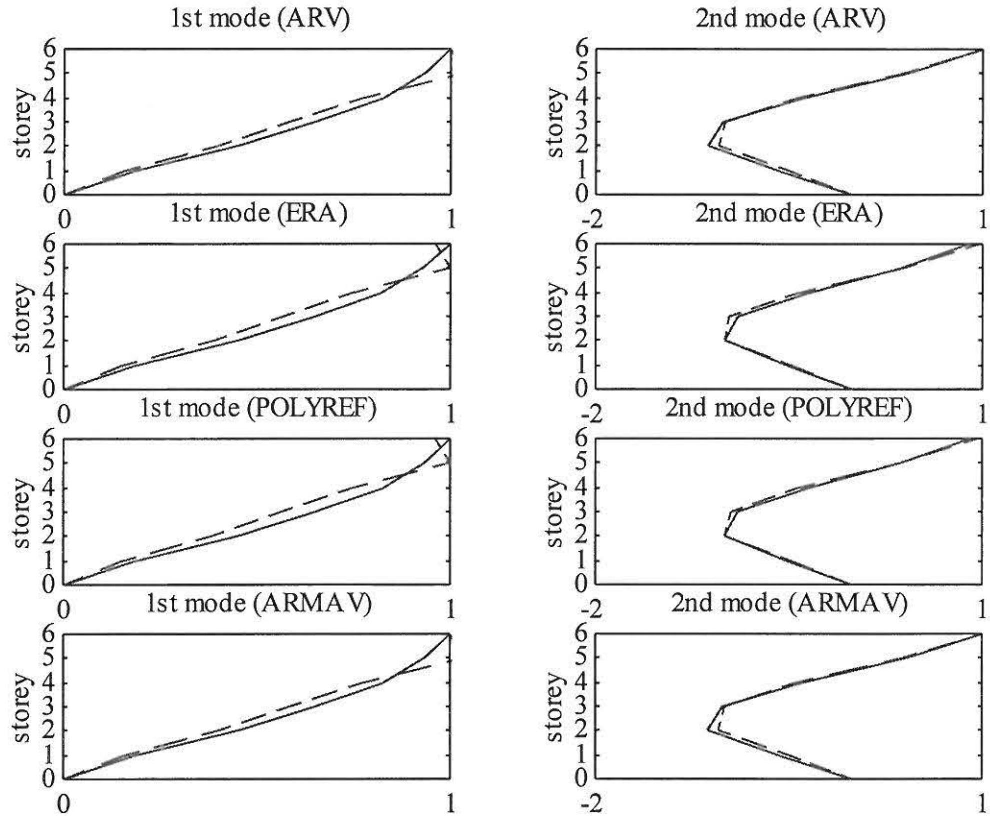

Figure 5.10 Identified mode shapes of the frame structure AAU3 after EQ2 (fd3_b11.dat). Load = 75 kg. [———] : Virgin state, [- - - - -]: damaged structure.

SI-method	f_1 [Hz]	f_2 [Hz]	ζ_1 [%]	ζ_2 [%]
ARV	1.415	4.551	4.57	3.24
ERA	1.396	4.559	4.12	3.59
POYLREF	1.407	4.566	4.17	3.55
ARMAV	1.412	4.552	4.11	3.37

Table 5.12 Identified frequencies and damping ratios of the frame structure AAU3 after EQ3 (fd3_b13.dat). Load = 50 kg.

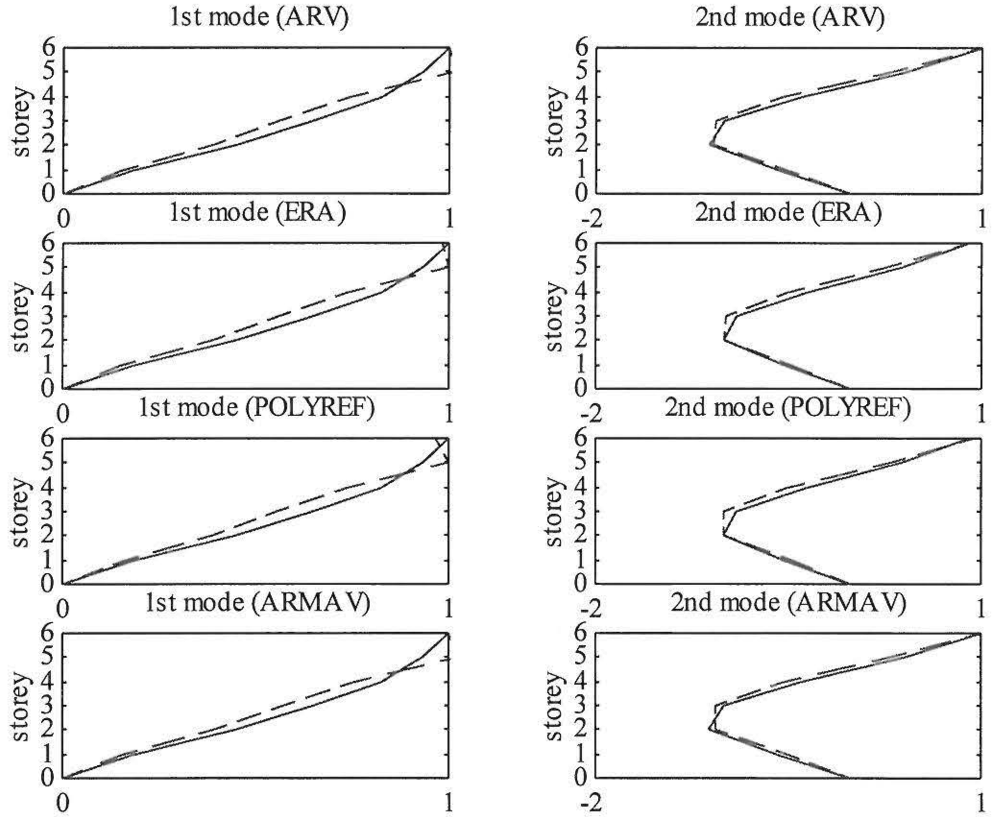

Figure 5.11 Identified mode shapes of the frame structure AAU3 after EQ3 (fd3_b13.dat). Load = 50 kg. [————] : Virgin state, [- - - - -]: damaged structure.

SI-method	f_1 [Hz]	f_2 [Hz]	ζ_1 [%]	ζ_2 [%]
ARV	1.376	4.454	4.42	3.14
ERA	1.362	4.401	4.09	3.58
POYLREF	1.370	4.438	4.19	3.67
ARMAV	1.375	4.458	4.62	3.27

Table 5.13 Identified frequencies and damping ratios of the frame structure AAU3 after EQ3 (fd3_b14.dat). Load = 75 kg.

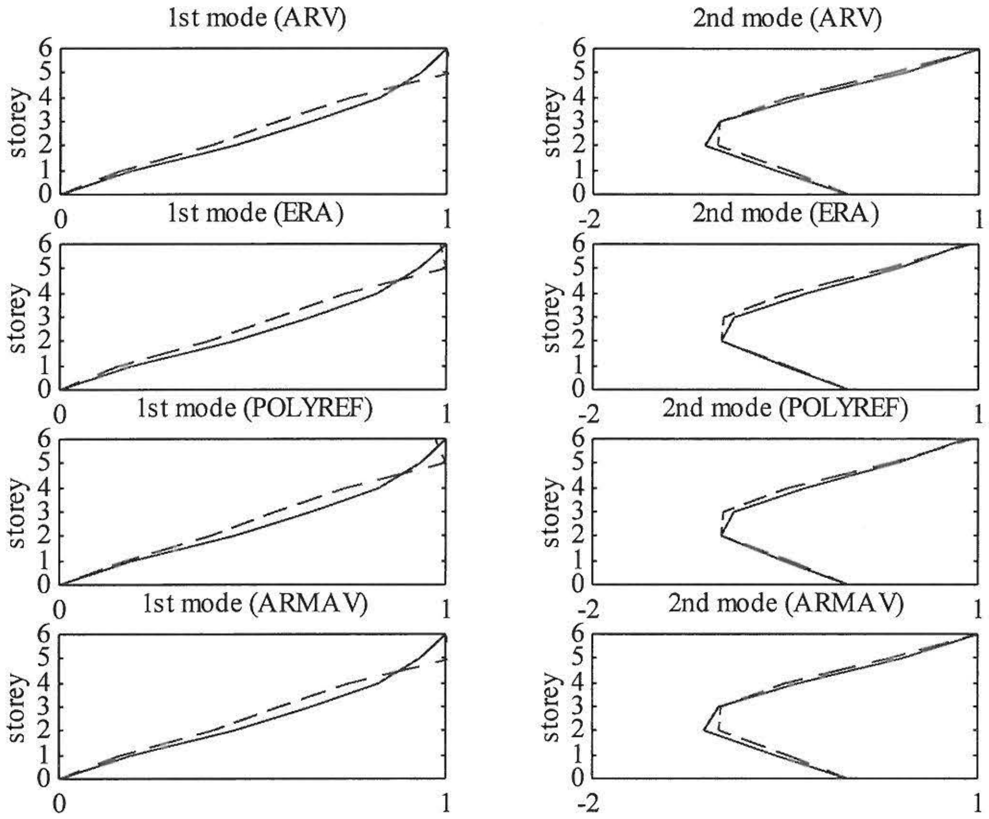

Figure 5.12 Identified mode shapes of the frame structure AAU3 after EQ3 (fd3_b14.dat). Load = 75 kg. [———] : Virgin state, [- - - - -]: damaged structure.

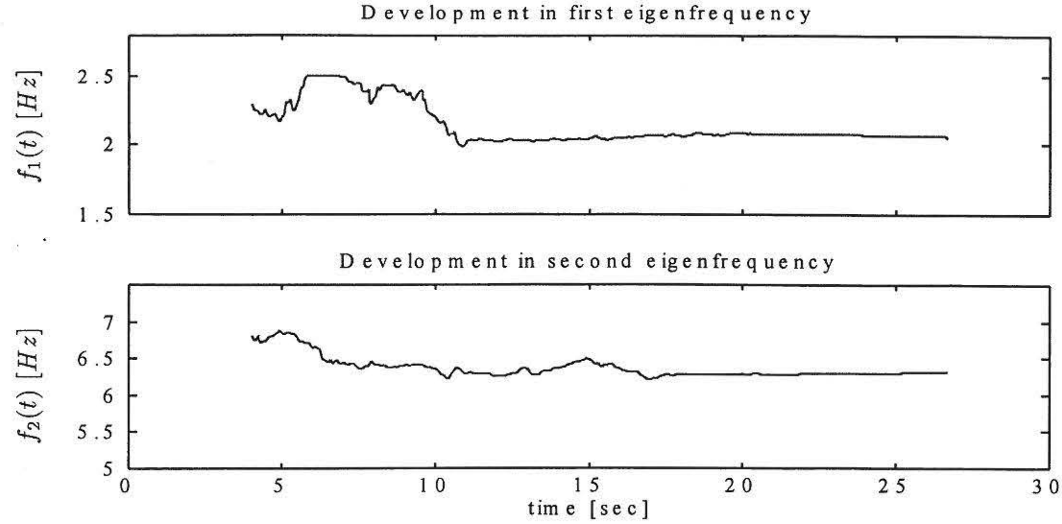

Figure 5.13 Development of softning in first and second mode during EQ1

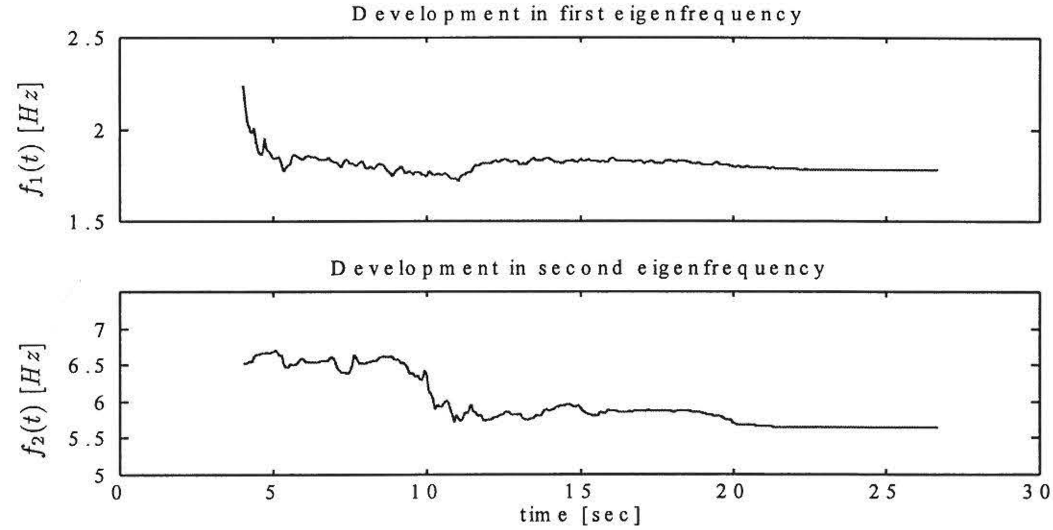

Figure 5.14 Development of softning in first and second mode during EQ2

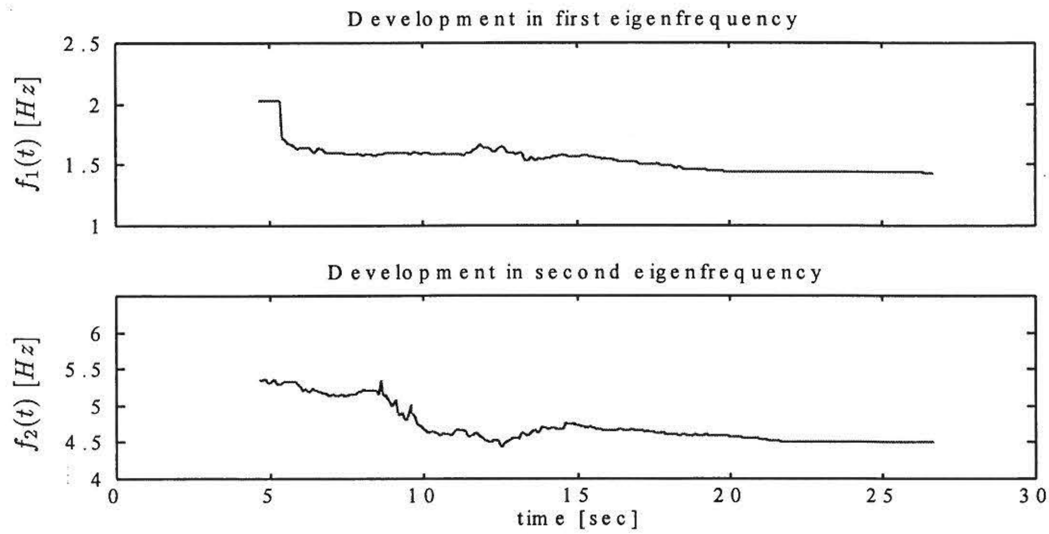

Figure 5.15 Development of softning in first and second mode during EQ3

6 SUMMARY OF RESULTS

In this chapter the results presented in chapters 3, 4 and 5, respectively will be summarised and comments are given.

6.1 Results from frame AAU1

From table 3.1 it is seen that 11 free decay measurements, 5 weak motion measurements and 3 strong motion measurements were performed with frame AAU1. Three free decay and three weak earthquake tests were performed before the first strong earthquake test in order to make a virgin state identification of the frame. The free-decay tests were performed by pulling a rope attached to the top storey beams. The following measurement sessions consisted of one strong motion measurement, one weak motion measurement and 2 free decay measurements. The identification results in tables 3.1 - 3.7 show a good aggreement for the different identification techniques. A decrease in the natural frequencies and an increase in the damping ratios are observed as expected for increasing damage level. However, it is seen that the second damping ratio is more uncertain determined than the first damping ratio. The reason for this can be that most energy is concentrated in the first mode by relasing the rope. The weak motion results in table 3.5 show frequency and damping ratio estimates which differ a little from the free decay results which can be due to that the excitation levels are different in the two . By comparing the free deacy results with the strong motion test results (final softening) in figures 3.11 - 3.13 a good harmony is observed. Figure 3.11 also shows a very fluctuating estimation of the development in the two lowest natural frequencies during the earthquake due to intense damage development. The mode shape estimates shown in figures 3.5 - 3.10 show only a little change for increasing damage level in the first mode while no changes can be observed in the second mode.

6.2 Results from frame AAU2

From table 4.1 it is seen that 8 free decay measurements, 5 weak motion measurements and 2 strong motion measurements were performed with AAU2. Three free decay and three weak earthquake tests were performed before the first strong earthquake test in order to make a virgin state identification of the frame. The free-decay tests were performed by means of a excitation set-up implying that the pull-out force could be measured. The following measurement sessions consisted of one strong motion measurement, one weak motion measurement and 1 free decay measurements. It should be noticed that the frame AAU2 was restricted to move out of the plane after it was found that the frame AAU1 made rotation vibrations during the tests.
By considering the identification results in tables 4.1 - 4.11 it can be concluded that a good aggreement for the different identification techniques exists. A decrease in the natural frequencies and an increase in the damping ratios are observed as expected for increasing damage level. It is seen that the the second damping ratio is determined with less uncertatinty than for frame AAU1. This is a due to use of a more well defined excitation than used for frame AAU1. Table 4.8 - 4.10 also show that the free decay results are sensitive to the pull-out load, i.e. excitation level. By comparing the free decay results with the strong motion test results (final softening) in figures 4.9 - 4.10 a good agreement is observed.
The mode shape estimates shown in figures 4.1 - 4.8 show a little change for increasing damage level in both the first mode and the second mode.

6.3 Results from frame AAU3

From table 5.1 it is seen that 14 free decay measurements and 3 strong motion measurements were performed. It should be noticed that the frame AAU3 was restricted to move in the plane as frame AAU2. Further, frame AAU3 was not tested by weak earthquake motion.
The results obtained from frame AAU3 show same tendency as observed for frame AAU1 and AAU2, respectively. However, the mode shape estimates shown in figures 5.1 - 5.12 indicates an other damage pattern of frame AAU3 than of frame AAU1 and AAU2, respectively. This is due to that earthquake type b, see figure 3.1 has a different energy content than the earthquake of type a which has been used in the tests of frame AAU1 and AAU2.

7 ACKNOWLEDGEMENTS

The present research was partially supported by The Danish Technical Research Council within the project: Dynamics of Structures.

8 REFERENCES

[1] Skjærbæk, P.S., Nielsen, S.R.K. & Kirkegaard, P.H. Earthquake Tests on Scale 1:5 RC-frame. Fracture & Dynamics Paper No. 86, Aalborg University, 1997.

[2] Pandit, S. W. & N. P. Metha Data Dependent Systems Approach to Modal Analysis Via State Space. ASME paper No. 85-WA/DSC-1, 1985.

[3] Juang, J.-N. Applied System Identification, Prentice Hall, 1994.

[4] Vold, H. & Crowley, J. A Modal Confidence Factor for the Polyreference Method. Proc. 3rd International Modal Analysis Conference, pp. 305-310, 1984.

[5] Kirkegaard, P.H., Andersen. P. & Brincker, R. Identification of Civil Engineering Structures using Multivariate Armav and Rarmav Models. Presented at the International Conference on Identification in Engineering Systems, Swansea, 27 -29 March, 1996.

FRACTURE AND DYNAMICS PAPERS

PAPER NO. 61: R. Brincker, P. Andersen, P. H. Kirkegaard, J. P. Ulfkjær: *Damage Detection in Laboratory Concrete Beams.* ISSN 0902-7513 R9458.

PAPER NO. 62: R. Brincker, J. Simonsen, W. Hansen: *Some Aspects of Formation of Cracks in FRC with Main Reinforcement.* ISSN 0902-7513 R9506.

PAPER NO. 63: R. Brincker, J. P. Ulfkjær, P. Adamsen, L. Langvad, R. Toft: *Analytical Model for Hook Anchor Pull-out.* ISSN 0902-7513 R9511.

PAPER NO. 64: P. S. Skjærbæk, S. R. K. Nielsen, A. Ş. Çakmak: *Assessment of Damage in Seismically Excited RC-Structures from a Single Measured Response.* ISSN 1395-7953 R9528.

PAPER NO. 65: J. C. Asmussen, S. R. Ibrahim, R. Brincker: *Random Decrement and Regression Analysis of Traffic Responses of Bridges.* ISSN 1395-7953 R9529.

PAPER NO. 66: R. Brincker, P. Andersen, M. E. Martinez, F. Tallavó: *Modal Analysis of an Offshore Platform using Two Different ARMA Approaches.* ISSN 1395-7953 R9531.

PAPER NO. 67: J. C. Asmussen, R. Brincker: *Estimation of Frequency Response Functions by Random Decrement.* ISSN 1395-7953 R9532.

PAPER NO. 68: P. H. Kirkegaard, P. Andersen, R. Brincker: *Identification of an Equivalent Linear Model for a Non-Linear Time-Variant RC-Structure.* ISSN 1395-7953 R9533.

PAPER NO. 69: P. H. Kirkegaard, P. Andersen, R. Brincker: *Identification of the Skirt Piled Gullfaks C Gravity Platform using ARMAV Models.* ISSN 1395-7953 R9534.

PAPER NO. 70: P. H. Kirkegaard, P. Andersen, R. Brincker: *Identification of Civil Engineering Structures using Multivariate ARMAV and RARMAV Models.* ISSN 1395-7953 R9535.

PAPER NO. 71: P. Andersen, R. Brincker, P. H. Kirkegaard: *Theory of Covariance Equivalent ARMAV Models of Civil Engineering Structures.* ISSN 1395-7953 R9536.

PAPER NO. 72: S. R. Ibrahim, R. Brincker, J. C. Asmussen: *Modal Parameter Identification from Responses of General Unknown Random Inputs.*ISSN 1395-7953 R9544.

PAPER NO. 73: S. R. K. Nielsen, P. H. Kirkegaard: *Active Vibration Control of a Monopile Offshore Structure. Part One - Pilot Project.* ISSN 1395-7953 R9609.

PAPER NO. 74: J. P. Ulfkjær, L. Pilegaard Hansen, S. Qvist, S. H. Madsen: *Fracture Energy of Plain Concrete Beams at Different Rates of Loading.* ISSN 1395-7953 R9610.

PAPER NO 75: J. P. Ulfkjær, M. S. Henriksen, B. Aarup: *Experimental Investigation of the Fracture Behaviour of Reinforced Ultra High Strength Concrete.* ISSN 1395-7953 R9611.

PAPER NO. 76: J. C. Asmussen, P. Andersen: *Identification of EURO-SEIS Test Structure.* ISSN 1395-7953 R9612.

PAPER NO. 77: P. S. Skjærbæk, S. R. K. Nielsen, A. Ş. Çakmak: *Identification of Damage in RC-Structures from Earthquake Records - Optimal Location of Sensors.* ISSN 1395-7953 R9614.

FRACTURE AND DYNAMICS PAPERS

PAPER NO. 78: P. Andersen, P. H. Kirkegaard, R. Brincker: *System Identification of Civil Engineering Structures using State Space and ARMAV Models.* ISSN 1395-7953 R9618.

PAPER NO. 79: P. H. Kirkegaard, P. S. Skjærbæk, P. Andersen: *Identification of Time Varying Civil Engineering Structures using Multivariate Recursive Time Domain Models.* ISSN 1395-7953 R9619.

PAPER NO. 80: J. C. Asmussen, R. Brincker: *Estimation of Correlation Functions by Random Decrement.* ISSN 1395-7953 R9624.

PAPER NO. 81: M. S. Henriksen, J. P. Ulfkjær, R. Brincker: *Scale Effects and Transitional Failure Phenomena of Reinforced concrete Beams in Flexure. Part 1.* ISSN 1395-7953 R9628.

PAPER NO. 82: P. Andersen, P. H. Kirkegaard, R. Brincker: *Filtering out Environmental Effects in Damage Detection of Civil Engineering Structures.* ISSN 1395-7953 R9633.

PAPER NO. 83: P. S. Skjærbæk, S. R. K. Nielsen, P. H. Kirkegaard, A. Ş. Çakmak: *Case Study of Local Damage Indicators for a 2-Bay, 6-Storey RC-Frame subject to Earthquakes.* ISSN 1395-7953 R9639.

PAPER NO. 84: P. S. Skjærbæk, S. R. K. Nielsen, P. H. Kirkegaard, A. Ş. Çakmak: *Modal Identification of a Time-Invariant 6-Storey Model Test RC-Frame from Free Decay Tests using Multi-Variate Models.* ISSN 1395-7953 R9640.

PAPER NO. 85: P. H. Kirkegaard, P. S. Skjærbæk, S. R. K. Nielsen: *Identification Report: Earthquake Tests on 2-Bay, 6-Storey Scale 1:5 RC-Frames.* ISSN 1395-7953 R9703.

PAPER NO. 89: P. S. Skjærbæk, P. H. Kirkegaard, S. R. K. Nielsen: *Shaking Table Tests of Reinforced Concrete Frames.* ISSN 1395-7953 R9704.

PAPER NO. 91: P. S. Skjærbæk, P. H. Kirkegaard, G. N. Fouskitakis, S. D. Fassois: *Non-Stationary Modelling and Simulation of Near-Source Earthquake Ground Motion: ARMA and Neural Network Methods.* ISSN 1395-7953 R9641.

PAPER NO. 92: J. C. Asmussen, S. R. Ibrahim, R. Brincker: *Application of Vector Triggering Random Decrement.* ISSN 1395-7953 R9634.

PAPER NO. 93: S. R. Ibrahim, J. C. Asmussen, R. Brincker: *Theory of Vector Triggering Random Decrement.* ISSN 1395-7953 R9635.

PAPER NO. 94: R. Brincker, J. C. Asmussen: *Random Decrement Based FRF Estimation.* ISSN 1395-7953 R9636.

PAPER NO. 95: P. H. Kirkegaard, P. Andersen, R. Brincker: *Structural Time Domain Identification (STDI) Toolbox for Use with MATLAB.* ISSN 1395-7953 R9642.

PAPER NO. 96: P. H. Kirkegaard, P. Andersen: *State Space Identification of Civil Engineering Structures from Output Measurements.* ISSN 1395-7953 R9643.

PAPER NO. 97: P. Andersen, P. H. Kirkegaard, R. Brincker: *Structural Time Domain Identification Toolbox - for Use with MATLAB.* ISSN 1395-7953 R9701.

Department of Building Technology and Structural Engineering
Aalborg University, Sohngaardsholmsvej 57, DK 9000 Aalborg
Telephone: +45 98 15 85 22 Telefax: +45 98 14 82 43